Dissipative phase fluctuations in superconducting wires capacitively coupled to diffusive metals

Alejandro M. Lobos and Thierry Giamarchi
DPMC-MaNEP, University of Geneva, 24 Quai Ernest-Ansermet, CH-1211 Geneva, Switzerland
(Received 25 April 2010; revised manuscript received 16 July 2010; published 22 September 2010)

We study the screening of the Coulomb interaction in a quasi-one-dimensional superconductor by the presence of either a one- or a two-dimensional electron gas nearby. To that end, we derive an effective low-energy phase-only action, which amounts to treating the Coulomb and superconducting correlations in the random-phase approximation. We concentrate on the study of dissipation effects in the superconductor, induced by the effect of Coulomb coupling to the diffusive modes in the electron gas, and study its consequences on the behavior of the one-dimensional plasma mode, and the static and dynamical conductivity. Our results point toward the importance of the dimensionality of the screening metal in the behavior of the superconducting plasma mode of the wire at low energies. In absence of topological defects, and when the screening is given by a one-dimensional electron gas, the superconducting plasma mode is completely damped in the limit $k \to 0$, and consequently superconductivity is lost in the wire. In contrast, we recover a Drude-type response in the conductivity when the screening is provided by a two-dimensional electron gas.

DOI: 10.1103/PhysRevB.82.104517 PACS number(s): 74.78.−w, 74.25.N−, 74.25.Gz

I. INTRODUCTION

The environment has profound effects on the properties of quantum systems.[1] In the case of superconductors, it was predicted more than 25 years ago that a resistively shunted Josephson junction would experience a superconductor-normal transition as a function of R_S/R_Q, where R_S is the shunt resistance of the junction and $R_Q=h/4e^2 \approx 6.45$ kΩ is the quantum of resistance.[2–4] More recently, a variety of superconducting systems, including granular,[5] or homogeneous[6] films, two-dimensional (2D) Josephson junctions arrays,[7] out-of-equilibrium Josephson junctions,[8] and high-temperature superconductors[9] were shown to undergo a superconductor-insulator transition as the characteristic resistance of the system in the normal state increases through a critical value on the order of R_Q. In those cases, the dissipative environment corresponds to the measurement circuits or the intrinsic component of normal electrons in the system.

In contrast, isolated superconducting wires with lateral dimension $r_0 \ll \xi_0$, where ξ_0 is the bulk coherence length, do not present significant dissipation sources at low temperatures. The low-energy modes in an ideally isolated superconducting wire are the one-dimensional (1D) propagating plasma modes along the axis.[10] Contrary to bulk superconductors, where the plasmon has an energy $\omega_p^{3D}=\sqrt{4\pi n_s e^2/m}$ (where n_s is the superfluid density and m is the electron mass), in the restricted 1D geometry of the wire, the long-ranged Coulomb interaction is not completely screened and consequently charge fluctuations are not shifted to finite energies in the limit $k \to 0$. The result is a soundlike dispersion relation $\omega^2(k) \sim k^2 \ln(1/kr_0)$, where the logarithmic factor is a remnant of the long-range interaction. Because of the gapless dispersion relation, quantum fluctuations are expected to show critical behavior,[11] a feature that has attracted the attention of several theoretical[12–15] and experimental[16–18] research groups.

How this picture (i.e., soundlike dispersion relation and critical behavior) is modified when the coupling to the electromagnetic environment is taken into account? Intuitively, the presence of a metal at a distance d should screen the Coulomb interaction for density fluctuations with wavelength $k \ll d^{-1}$, resulting in enhanced superconducting correlations.[11] On the other hand, in capacitively coupled superconductor-normal systems, the presence of dissipation in the normal metal (e.g., presence of impurities) is known to produce dissipative order-parameter fluctuations[19–22] and, from this point of view, screening might also be accompanied by detrimental effects to superconductivity. Indeed, recent theoretical works on related Luttinger-liquid systems coupled electrostatically to metals predict charge-density wave and other instabilities caused by the dissipative environment, which destroy the superconducting state.[23,24]

Therefore, a better understanding of the screening effects occurring in superconducting wires and the consequences to their superconducting properties is needed. This issue is particularly relevant to recent theoretical[13,25,26] and experimental[27,28] works showing evidence of stabilization of superconductivity in low-dimensional systems due to the presence of tunneling contacts with normal metallic leads, which suppress fluctuations of the superconducting order parameter. It would be desirable to investigate to what extent the same leads introduce additional sources of dissipation prejudicial to superconductivity.

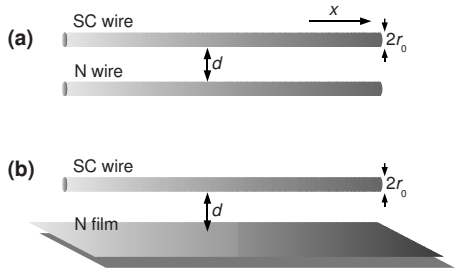

FIG. 1. Representation of the capacitively coupled superconducting-wire-normal-metal system. The metal placed at a distance d screens the long-range Coulomb interaction in the superconducting wire. In (a) the metal is a diffusive wire and in (b) we consider a diffusive 2D electron gas.

In this paper we study the effects of the screening of the Coulomb interaction in a quasi-1D superconductor by the presence of a metal nearby (cf. Fig. 1). To that end, we derive an effective model (i.e., phase-only action) of the coupled system valid at low energies, which amounts to performing the so-called random-phase approximation (RPA) of the interacting problem.

We specify two experimentally relevant geometries, namely: (a) a 1D and (b) a 2D electron gas (1DEG and 2DEG, respectively) in the diffusive limit. Our results show a rich behavior of the 1D plasma mode in the wire due to screening and dissipative effects, and point toward the importance of the dimensionality of the screening metal. In particular, in the case of screening provided by a 1DEG, important frictional effects are observed in the superconductor due to the capacitive coupling. In that case, due to their slow diffusive motion, electrons in the 1DEG are unable to screen out the faster density fluctuations associated with the 1D plasmon,[19] and in the limit $k\to 0$ and $T\to 0$ phase coherence is destroyed and the wire shows a finite residual resistivity. In contrast, for a wire coupled to a 2DEG, screening is more efficient due to the additional transverse degree of freedom in the plane. As a consequence, dissipation vanishes in the limit $k\to 0$, and the wire is well described by the Luttinger-liquid picture.

The paper is divided as follows: in Sec. II we derive a general effective phase-only action for the coupled superconductor-normal system and derive the equation of motion for the 1D plasma mode, in Sec. III we present a detailed analysis of the screening regimes at low energies for both the 1D and 2D geometries, Sec. IV is devoted to the study of the dissipative effects in the dynamical conductivity $\sigma(k,\omega)$ of the wire, and finally in Sec. V we summarize our findings and present a discussion. The details of the derivation of the low-energy effective action are given in Appendices A and B.

II. MODEL

In this section we derive a general effective model which describes a clean superconducting wire of length L capacitively coupled to a diffusive metal, and present a general formalism to obtain the dispersion relation of the 1D plasmon. The derivation of the model is standard[12,21,29,30] and here we only sketch the main steps. We refer the reader to Appendix A and to the aforementioned references for details.

In the following we use the convention $\hbar=k_B=1$. We begin our description with the microscopic action of the complete system depicted in Fig. 1,

$$S=\int_0^\beta d\tau\sum_{a,\sigma}\int d\mathbf{r}\psi^*_{a,\sigma}(\partial_\tau-\mu_a)\psi_{a,\sigma}+\int_0^\beta d\tau H, \qquad (1)$$

where $\beta=\frac{1}{T}$. The Grassmann field $\psi_{a,\sigma}\equiv\psi_{a,\sigma}(\mathbf{r},\tau)$ describes an electron in the superconductor for $a=s$ (normal metal for $a=n$) with spin projection σ at position $\mathbf{r}\equiv(x,y,z)$ and imaginary time τ. The chemical potential $\mu_a=k^2_{\mathrm{F},a}/2m$ is the Fermi energy in the normal state with $k_{\mathrm{F},a}$ the Fermi wave vector. The Hamiltonian H of the systems is

$$H=H^0_{\mathrm{s}}+H^0_{\mathrm{n}}+H_{\mathrm{int}}, \qquad (2)$$

where

$$H^0_{\mathrm{s}}=\int d\mathbf{r}\sum_\sigma\frac{[\nabla\psi^\dagger_{s,\sigma}][\nabla\psi_{s,\sigma}]}{2m}+U\psi^\dagger_{s\uparrow}\psi^\dagger_{s\downarrow}\psi_{s\downarrow}\psi_{s\uparrow}, \qquad (3)$$

describes a translationally invariant, clean superconductor. Since we will not focus on the details of the pairing mechanism, here we assume a phenomenological local attractive interaction $U<0$ which is responsible for (s-wave) pairing at $T<T_c$.

The normal metal is described by

$$H^0_{\mathrm{n}}=\int d\mathbf{r}\sum_\sigma\left\{\frac{[\nabla\psi^\dagger_{n,\sigma}][\nabla\psi_{n,\sigma}]}{2m}+\psi^\dagger_{n,\sigma}V_i\psi_{n,\sigma}\right\}, \qquad (4)$$

where $V_i\equiv V_i(\mathbf{r})$ represents the weak static impurity potential which provides a finite resistivity in the metal.

Finally, the interaction term is

$$\begin{aligned}H_{\mathrm{int}}=&\frac{1}{2}\int d\mathbf{r}_1d\mathbf{r}_2\hat\rho_s(\mathbf{r}_1)v(\mathbf{r}_1-\mathbf{r}_2,0)\hat\rho_s(\mathbf{r}_2)\\&+\frac{1}{2}\int d\mathbf{r}_1d\mathbf{r}_2\hat\rho_n(\mathbf{r}_1)v(\mathbf{r}_1-\mathbf{r}_2,0)\hat\rho_n(\mathbf{r}_2)\\&+\int d\mathbf{r}_1d\mathbf{r}_2\hat\rho_s(\mathbf{r}_1)v(\mathbf{r}_1-\mathbf{r}_2,d)\hat\rho_n(\mathbf{r}_2),\end{aligned} \qquad (5)$$

where we defined the electronic density operators $\hat\rho_a(\mathbf{r})\equiv\Sigma_\sigma\psi^\dagger_{a,\sigma}(\mathbf{r})\psi_{a,\sigma}(\mathbf{r})$, and where the domain of integration of the variables $\mathbf{r}_1$ and $\mathbf{r}_2$ is constrained to the volume of the superconductor (for $a=s$) and the metal (for $a=n$). The particular geometry of the system (cf. Fig. 1) allows us to write the microscopic long-range Coulomb interaction potential as

$$v(\mathbf{r}_1-\mathbf{r}_2,d)=\frac{1}{\epsilon_{\mathrm{r}}}\frac{e^2}{\sqrt{|\mathbf{r}_1-\mathbf{r}_2|^2_{xy}+d^2}}, \qquad (6)$$

where $|\mathbf{r}_1-\mathbf{r}_2|_{xy}$ and d are the distances between coordinates $\mathbf{r}_1$ and $\mathbf{r}_2$ in the xy plane and along the z axis, respectively, and ϵ_{r} is the dielectric constant of the insulating medium between the metal and the superconductor.

The first step in the derivation of an effective low-energy model consists in decoupling the interaction terms appearing in H^0_{s} and H_{int} by the means of suitable Hubbard-Stratonovich transformations (HSTs). The repulsive Coulomb interaction H_{int} is more conveniently decoupled by expressing it in terms of the symmetric and antisymmetric density operators (cf. Appendix A),

$$\hat\rho_\pm(\mathbf{r})\equiv\hat\rho_s(\mathbf{r})\pm\hat\rho_n(\mathbf{r}). \qquad (7)$$

With this definition, the interaction term [cf. Eq. (5)] compactly writes

$$H_{\mathrm{int}}=\frac{1}{2}\sum_{\nu=\pm}\int d\mathbf{r}_1d\mathbf{r}_2\hat\rho_\nu(\mathbf{r}_1)v_\nu(\mathbf{r}_1-\mathbf{r}_2)\hat\rho_\nu(\mathbf{r}_2), \qquad (8)$$

where

$$v_\nu(\mathbf{r}) \equiv \frac{v(\mathbf{r},0) + (\nu)v(\mathbf{r},d)}{2} \quad (\text{with } \nu = \pm). \tag{9}$$

The HS transformations to decouple the Coulomb and the Hubbard $U<0$ interactions are implemented by introducing the HS fields $\tilde{\rho}_\nu(\mathbf{r},\tau)$ in the particle-hole channel, and $\Delta^*(\mathbf{r},\tau)$, $\Delta(\mathbf{r},\tau)$ in the particle-particle channel, respectively (cf. Appendix A).

The next step in our derivation is to introduce an extra HS field $\rho_\nu(\mathbf{r},\tau)$ in order to decouple the quadratic term in $\tilde{\rho}_\nu(\mathbf{r},\tau)$, appearing in Eq. (A1). Then, it is easy to show that the field $\tilde{\rho}_\nu(\mathbf{r},\tau)$ can be formally integrated out, yielding a functional-delta function[31] $\delta[\hat{\rho}_\nu(\mathbf{r},\tau) - \rho_\nu(\mathbf{r},\tau)]$. As noted by De Palo *et al.*,[21] this fact allows to interpret the new HS fields $\rho_\nu(\mathbf{r},\tau)$ as the *physical density* of the problem, expressed in our case in terms of the symmetric and antisymmetric collective modes.

At $T \ll T_c$, amplitude fluctuations of the order parameter $\Delta(\mathbf{r},\tau)$ can be neglected, allowing to write $\Delta(\mathbf{r},\tau) = \Delta_0 e^{i\theta(\mathbf{r},\tau)}$, with a real constant Δ_0 representing the BCS mean-field gap energy. The phase field $\theta(\mathbf{r},\tau)$ can be absorbed by a unitary transformation of the fermionic field,[21]

$$\psi_{s,\sigma}(\mathbf{r},\tau) \to \psi'_{s,\sigma}(\mathbf{r},\tau) = \psi_{s,\sigma}(\mathbf{r},\tau) e^{i\theta(\mathbf{r},\tau)/2}.$$

The derivation of the effective model proceeds with the integration of the fermionic fields $\psi_{a,\sigma}$, and the expansion of the resulting bosonic action around the saddle-point in terms of derivatives of $\theta(\mathbf{r},\tau)$ and density fluctuations $\delta\tilde{\rho}_\nu(\mathbf{r},\tau)$, $\delta\rho_\nu(\mathbf{r},\tau)$ [cf. Eqs. (A10) and (A11)]. This expansion amounts to performing the RPA approximation of the interacting problem.[21,32]

Then we integrate the auxiliary field $\delta\tilde{\rho}_\nu(\mathbf{r},\tau)$, which in the original representation of the density in terms of the fields $\delta\rho_s(\mathbf{r},\tau)$, $\delta\rho_n(\mathbf{r},\tau)$ yields

$$\begin{aligned} S_{\text{eff}} = & \int d\mathbf{r} d\tau \frac{i}{2} \partial_\tau \theta(\mathbf{r},\tau)\rho_s(\mathbf{r},\tau) + \frac{1}{2}\int d\mathbf{r}_1 d\mathbf{r}_2 d\tau_1 d\tau_2 \\ & \times [\nabla\theta(\mathbf{r}_1,\tau_1)\mathcal{D}(\mathbf{r}_1-\mathbf{r}_2,\tau_1-\tau_2)\nabla\theta(\mathbf{r}_2,\tau_2) \\ & + \boldsymbol{\delta\rho}^\dagger(\mathbf{r}_1,\tau_1)\hat{\boldsymbol{\chi}}^{-1}(\mathbf{r}_1-\mathbf{r}_2,\tau_1-\tau_2)\boldsymbol{\delta\rho}(\mathbf{r}_2,\tau_2)]. \end{aligned} \tag{10}$$

In this expression, $\mathcal{D}(\mathbf{r},\tau)$ is the phase stiffness of the superconductor [cf. Eq. (A15)], which physically measures the tendency of the wire to have a uniform phase field $\theta(\mathbf{r},\tau)$. $\boldsymbol{\delta\rho}(\mathbf{r},\tau)$ is the vector of densities,

$$\boldsymbol{\delta\rho}(\mathbf{r},\tau) \equiv \begin{pmatrix} \delta\rho_s(\mathbf{r},\tau) \\ \delta\rho_n(\mathbf{r},\tau) \end{pmatrix}$$

and $\hat{\boldsymbol{\chi}}(\mathbf{r},\tau)$ is the RPA density-response matrix, which characterizes the response of the charge $\boldsymbol{\delta\rho}(\mathbf{r},\tau)$ due to an external potential $\boldsymbol{\varphi}(\mathbf{r},\tau)$: $\boldsymbol{\delta\rho}(\mathbf{r},\tau) = -\int d\mathbf{r}' d\tau' \hat{\boldsymbol{\chi}}(\mathbf{r}-\mathbf{r}', \tau-\tau')\boldsymbol{\varphi}(\mathbf{r}',\tau')$, and contains all the information about screening and interaction between the superconductor and the electron gas [cf. Eq. (A15)].

The above action, Eq. (10), is more conveniently expressed in Fourier space as

$$\begin{aligned} S_{\text{eff}} = & \frac{1}{2\beta V}\sum_{\mathbf{k},\omega_m} \omega_m \theta^*(\mathbf{k},\omega_m)\rho_s(\mathbf{k},\omega_m) \\ & + [k^2|\theta(\mathbf{k},\omega_m)|^2 \mathcal{D}(\mathbf{k},\omega_m) \\ & + \boldsymbol{\rho}^\dagger(\mathbf{k},\omega_m)\hat{\boldsymbol{\chi}}^{-1}(\mathbf{k},\omega_m)\boldsymbol{\rho}(\mathbf{k},\omega_m)], \end{aligned} \tag{11}$$

where $\mathbf{k}$ is the momentum and $\omega_m = \frac{2\pi m}{\beta}$ the bosonic Matsubara frequencies,[32] and where the representation of the fields

$$\theta(\mathbf{r},\tau) = \frac{1}{\beta V}\sum_{\mathbf{k},\omega_m} e^{i(\mathbf{k}.\mathbf{r}-\omega_m\tau)}\theta(\mathbf{k},\omega_m),$$

$$\delta\rho_a(\mathbf{r},\tau) = \frac{1}{\beta V}\sum_{\mathbf{k},\omega_m} e^{i(\mathbf{k}.\mathbf{r}-\omega_m\tau)}\rho_a(\mathbf{k},\omega_m),$$

has been used. In Fourier representation, the RPA density-response matrix is compactly written as

$$\hat{\boldsymbol{\chi}}(\mathbf{k},\omega_m) = \frac{1}{1+\hat{\boldsymbol{\chi}}_0(\mathbf{k},\omega_m)\hat{\mathbf{V}}_0(\mathbf{k})}\hat{\boldsymbol{\chi}}_0(\mathbf{k},\omega_m), \tag{12}$$

where

$$\hat{\boldsymbol{\chi}}_0(\mathbf{k},\omega_m) = \begin{bmatrix} \chi_{0,s}(\mathbf{k},\omega_m) & 0 \\ 0 & \chi_{0,n}(\mathbf{k},\omega_m) \end{bmatrix},$$

$$\hat{\mathbf{V}}_0(\mathbf{k}) = \begin{bmatrix} v(\mathbf{k},0) & v(\mathbf{k},d) \\ v(\mathbf{k},d) & v(\mathbf{k},0) \end{bmatrix}.$$

Here, the bare density-response functions $\chi_{0,s}(\mathbf{k},\omega_m)$ and $\chi_{0,n}(\mathbf{k},\omega_m)$ [cf. Eqs. (A12) and (A13)] are obtained from the Hamiltonians H_{s}^0 and H_{n}^0 [cf. Eqs. (3) and (4), respectively], and $v(\mathbf{k},d)$ is the Fourier transform of $v(\mathbf{r},d)$ in Eq. (6).

Note that at $T=0$ and in absence of quasiparticle excitations, the whole electronic density in the superconductor corresponds to the superfluid density. Consequently, the field $\delta\rho_s(\mathbf{r},\tau)$ physically represents the fluctuation of the Cooper-pair density at point $(\mathbf{r},\tau)$. An interesting aspect of the effective action in Eq. (10) is that the first term [i.e., coupling between the total density of Cooper pairs $\rho_s(\mathbf{r},\tau)$ and the phase field $\theta(\mathbf{r},\tau)$] appears naturally as a consequence of the well-known number-phase commutation relation $[\rho_s(\mathbf{r}), \theta(\mathbf{r}')] = i\delta(\mathbf{r}-\mathbf{r}')$ occurring in the superconducting ground state.[21,33]

The derivation of an effective model for the phase field $\theta(\mathbf{r},\tau)$ proceeds with the integration of the fields $\delta\rho_s(\mathbf{r},\tau)$ and $\delta\rho_n(\mathbf{r},\tau)$. When the superconductor is a very narrow wire of radius $r_0 \ll \xi_0$, the dependence of the fields $\theta(\mathbf{r},\tau)$, $\delta\rho_s(\mathbf{r},\tau)$ on transverse dimensions can be neglected, reducing to $\{\theta(\mathbf{r},\tau), \delta\rho_s(\mathbf{r},\tau)\} \to \{\theta(\mathbf{x}), \delta\rho_s(\mathbf{x})\}$ where the compact notation $\mathbf{x} \equiv (x,\tau)$ has been used (here x is the coordinate along the wire). Is also convenient to define the short-hand notation in Fourier representation $\mathbf{q} \equiv (k_\parallel, -\omega_m)$ with $k_\parallel$ the momentum parallel to the wire. Gaussian integration of the density fields $\delta\rho_s$ and $\delta\rho_n$ allows to obtain an effective model in terms of the phase field θ (i.e., "phase-only" action) of the superconducting wire screened by an effectively g-dimensional electron gas (g-DEG),

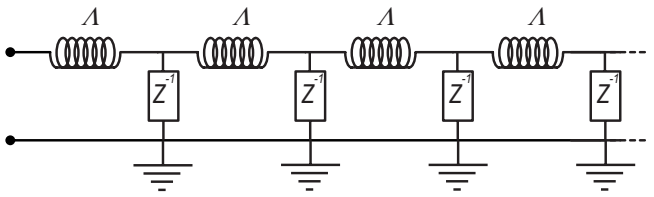

FIG. 2. Equivalent transmission-line circuit representing the superconducting wire capacitively coupled to the metallic environment. The kinetic inductance per unit of length Λ represents the dissipationless superconducting nature of the wire while the effective admittance $Z^{-1} \equiv Z^{-1}(k_\parallel, \omega)$ encodes all the capacitive and resistive effects arising from the coupling to the environment (cf. Fig. 1).

$$S^{\mathrm{w}}_{(g)} \simeq \frac{1}{2\beta L} \sum_{\mathbf{q}} \left\{ \frac{\omega_m^2}{4} \chi_s^{(g)}(\mathbf{q}) + q^2 \mathcal{D}(\mathbf{q}) \right\} |\theta(\mathbf{q})|^2, \quad (13)$$

where $\chi_s^{(g)}(\mathbf{q})$ is the RPA density-response function of the superconducting wire

$$\chi_s^{(g)}(\mathbf{q}) \equiv \frac{\chi_{0,s}(\mathbf{q})}{1 + \chi_{0,s}(\mathbf{q})[v^{(1)}(k_\parallel, 0) - v_{\mathrm{eff}}^{(g)}(\mathbf{q})]}. \quad (14)$$

Here $v^{(1)}(k_\parallel, d)$ is the 1D Fourier transform of the Coulomb potential, Eq. (6), (cutoff at short distances by the radius of the wire r_0),[11]

$$v^{(1)}(k_\parallel, d) = \frac{2e^2}{\epsilon_{\mathrm{r}}} K_0(|k_\parallel| \sqrt{r_0^2 + d^2}) \quad (15)$$

with $K_0(\zeta)$ the zeroth-order Bessel function, which verifies the limit $\lim_{\zeta \to 0} K_0(\zeta) \to -\ln(\frac{\zeta}{2})$ (cf. Ref. 34). The quantity $v_{\mathrm{eff}}^{(g)}(\mathbf{q})$ is an effective 1D (retarded) potential encoding all the information about screening provided by the g-DEG,

$$v_{\mathrm{eff}}^{(g)}(\mathbf{q}) \equiv \frac{1}{L_\perp^{g-1}} \sum_{\mathbf{k}_\perp} \frac{[v^{(g)}(k_\parallel, \mathbf{k}_\perp, d)]^2 \chi_{0,n}^{(g)}(\mathbf{q}, \mathbf{k}_\perp)}{1 + \chi_{0,n}^{(g)}(\mathbf{q}, \mathbf{k}_\perp) v^{(g)}(k_\parallel, \mathbf{k}_\perp, 0)}, \quad (16)$$

where we have introduced the notation $v^{(g)}(k_\parallel, \mathbf{k}_\perp, d)$ for the g-dimensional Fourier transform of the Coulomb potential, Eq. (6), in which we have explicitly splitted the spatial dependence into $k_\parallel$ and $\mathbf{k}_\perp$, the $(g-1)$-dimensional momentum perpendicular to the wire. Analogously, we have introduced the notation $\chi_{0,n}^{(g)}(\mathbf{q}, \mathbf{k}_\perp)$ for the density response function, Eq. (A13).

The minimization of the action $S_{(g)}^{w}$ [cf. Eq. (13)] allows to obtain the equation of motion of the field $\theta(\mathbf{q})$, from which the 1D plasma mode $\omega(k_\parallel)$ can be obtained in the limit $\mathbf{q} \to 0$, upon analytical continuation to real frequencies $i\omega_m \to \omega + i0^+$ (cf. Ref. 32),

$$-\frac{1}{4} \chi_s^{(g)}(k_\parallel, \omega + i0^+) \omega(k_\parallel)^2 + \mathcal{D}_0 k_\parallel^2 = 0, \quad (17)$$

where $\mathcal{D}_0 \equiv \lim_{\mathbf{q} \to 0} \mathcal{D}(\mathbf{q}) = \frac{\rho_s^{(0)}}{4m}$ (cf. Appendix B).

Note that the same dispersion relation for the 1D plasmon can be obtained using the equivalent transmission-line circuit depicted in Fig. 2. In this phenomenological description,[35] the dissipationless nature of the superconducting wire is represented by the kinetic inductance per unit of length Λ, while the effective admittance per unit of length $Z^{-1} = Z^{-1}(k_\parallel, \omega)$ encodes all the capacitive and resistive effects arising from the coupling to the metallic environment. These effective parameters are related to the microscopic theory by the relations,

$$\Lambda = \frac{1}{\mathcal{D}_0}, \quad (18)$$

$$Z^{-1}(k_\parallel, \omega) = -\frac{i\omega}{4} \chi_s^{(g)}(k_\parallel, \omega + i0^+). \quad (19)$$

In addition to the contribution of soft modes, encoded in Eq. (13), 1D superconductors exhibit stable topological excitations known as phase-slip excitations.[33,36,37] A phase slip is a region of size $\sim \xi_0$ where the order parameter temporarily vanishes, allowing the field $\theta(\mathbf{x})$ to perform a jump of $\pm 2\pi n$ (with n integer) across it, and can be understood as a vortex in 1+1 dimensions. For wires in the limit of very low superconducting stiffness, phase slips are an important source of momentum unbinding leading to finite resistivity for all temperatures below T_c, and a relevant perturbation to the action [in the renormalization-group (RG) sense].[11,12,38] Indeed, it is believed that at $T=0$, the eventual destruction of the superconducting state in isolated ultrathin wires occurs through the proliferation of quantum phase-slip/antiphase-slip pairs,[12,13,16–18,38–40] in what constitutes the quantum analog in 1+1 dimensions to the classical Berezinskii-Kosterlitz-Thouless (BKT) transition in 2D.[41]

Note that our derivation of Eq. (13) does not account for the presence of phase slips. Consequently, our results will only apply far from the BKT transition and far from the (nonsuperconducting) phase where the effect of phase slips dominates the low-energy properties. In the following we analyze the generic action of Eq. (10) for the different cases depicted in Fig. 1.

III. SCREENING REGIMES

A. Unscreened isolated wire

Let us first explore the instructive case of a superconducting wire ideally isolated from the environment. This situation corresponds to the normal metal placed infinitely far from the superconductor (i.e., $d \to \infty$), which results in the decoupling of their dynamics [i.e., $v_{\mathrm{eff}}^{(g)}(\mathbf{q}) \to 0$ in Eq. (14)]. From Eq. (14), the RPA density response is

$$\chi_s(\mathbf{q}) = \frac{\chi_{0,s}(\mathbf{q})}{1 + \chi_{0,s}(\mathbf{q}) v^{(1)}(k_\parallel, 0)} \underset{k_\parallel \to 0}{\to} \left[\frac{2e^2}{\epsilon_{\mathrm{r}}} \ln\left(\frac{2}{|k_\parallel r_0|} \right) \right]^{-1}. \quad (20)$$

Replacing this expression into Eq. (17) allows to obtain the equation of motion for the Mooij-Schön plasma mode,[10,11]

$$\omega^2(k_\parallel) - u^2(k_\parallel) k_\parallel^2 = 0 \quad (21)$$

with $u(k_\parallel) \equiv \sqrt{\frac{8e^2 \mathcal{D}_0}{\epsilon_{\mathrm{r}}} \ln(\frac{2}{|k_\parallel r_0|})}$ the (momentum-dependent) plasmon velocity.

Let us now concentrate on the superconducting properties of the wire. It is well-known that long-range order of the order parameter in 1D quantum systems is not possible, due to presence of strong quantum fluctuations and, strictly speaking, only quasi-long-range order, characterized by a slowly decreasing order-parameter correlation function,

$$F(\mathbf{x}) \equiv \langle \Delta^*(\mathbf{x})\Delta(0)\rangle = \Delta_0^2 e^{-(1/2)\langle T_\tau[\theta(\mathbf{x})-\theta(0)]^2\rangle}, \quad (22)$$

can exist.[11,42] In the case of the isolated wire, the phase-correlation function calculated with the effective phase-only action, Eq. (13), and the response $\chi_s(\mathbf{q})$, Eq. (20) writes[11,43]

$$\langle T_\tau[\theta(\mathbf{x})-\theta(0)]^2\rangle = \frac{1}{\pi K}\left[\ln\frac{\sqrt{x^2+u_0^2\tau^2}\ln\tau}{r_0}\right]^{3/2}, \quad (23)$$

where we have defined the (short-range) Luttinger interaction parameter K and the bare velocity u_0 as[11,43]

$$K \equiv \sqrt{\frac{\mathcal{D}_0\epsilon_r}{8e^2}}, \quad (24)$$

$$u_0 \equiv \sqrt{\frac{\mathcal{D}_0 8e^2}{\epsilon_r}}. \quad (25)$$

Compared to a 1D superconductor with short-range repulsive interactions,[11] the phase correlator of Eq. (23) yields a relatively faster decrease in the order-parameter correlation function, Eq. (22), as a consequence of the long-range Coulomb interaction which is not completely screened in the 1D geometry. Consequently, density fluctuations are suppressed in the limit $\mathbf{q}\to 0$ (cf. Ref. 43), and superconductivity, which benefits from fluctuations in the density, is suppressed.

A natural step to take in order to diminish the detrimental effects of the Coulomb interaction in the 1D geometry is to screen it by the means of a metal placed nearby. This is the subject of the subsequent sections.

B. Screening by a diffusive metallic wire

We now concentrate on the system depicted in Fig. 1(a). For simplicity, we consider the case of two geometrically identical cylindrical wires (extensions to other 1D geometries are straightforward). In the following we assume that the electron gas is only one-dimensional with respect to density fluctuations $\rho_n(\mathbf{q})$ with spatial wave vector $k_\parallel$ satisfying the condition $k_\parallel r_0 \ll 1$. Note that this condition does not necessarily imply that the normal wire is *electronically* 1D (i.e., it does not imply the existence of only one electronic conduction channel). Indeed, in the rest of this section we assume a normal metal with a large number of channels $N_{\rm ch} \sim (k_{F,n}r_0)^2 \gg 1$. This fact, together with the additional assumption of a very weak disorder potential, allows to neglect Anderson-localization effects (i.e., $L \ll \xi_{\rm wire}$, where $\xi_{\rm wire}$ is the localization length in the diffusive normal wire).

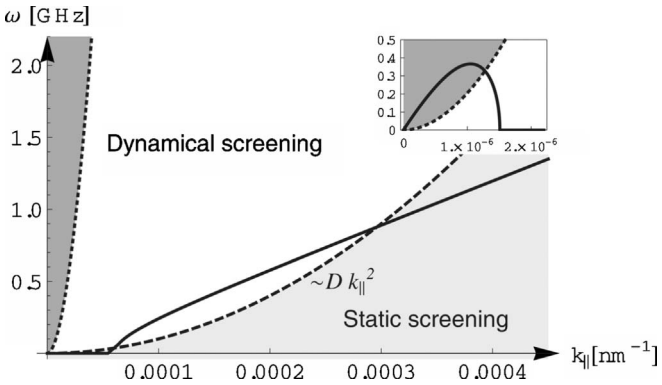

FIG. 3. Screening regimes for a superconducting wire screened by a diffusive 1DEG. The curve $\omega = Dk_\parallel^2$ (dashed line) separates the regime of static screening $\omega \ll Dk_\parallel^2$ (light gray area) from that of dynamical screening $\omega \gg Dk_\parallel^2$ (white area). The dispersion relation of the 1D plasma mode (thick solid line) is obtained from the numerical evaluation of Eq. (17), using Eq. (26) and the parameters in Table I. Note that the dispersion relation crosses over from the static regime to the dynamical regime and eventually the plasmon mode is completely damped. In the regime of frequencies $\omega \gg Dk_\parallel^2 \frac{2e^2}{\epsilon_r}\mathcal{N}_{n,1D}^0 \ln\frac{2}{|k_\parallel r_0|}$ (dark gray area) the unscreened Mooij-Schön plasma mode is recovered (see inset).

In the following we focus on the experimentally relevant regime $d \approx r_0 \ll k_\parallel^{-1}$. In that case $v^{(1)}(k_\parallel,0) \approx v^{(1)}(k_\parallel,d)$ and therefore the RPA-density response, Eq. (14), simplifies to

$$\chi_s^{(1)}(\mathbf{q}) \simeq \frac{\chi_{0,s}(\mathbf{q})[1+\chi_{0,n}^{(1)}(\mathbf{q})v(k_\parallel,0)]}{1+[\chi_{0,s}(\mathbf{q})+\chi_{0,n}^{(1)}(\mathbf{q})]v(k_\parallel,0)}. \quad (26)$$

For a weakly disordered diffusive electron gas with elastic mean-free path l_e and scattering time $\tau_e = l_e/v_{F,n}$, where $v_{F,n}$ is the Fermi velocity, the disorder-averaged density-response function [cf. Eq. (A13)] at energies $|\omega_m| < \tau_e^{-1}$ and momentum $q < l_e^{-1}$ writes[44]

$$\chi_{0,n}^{(1)}(\mathbf{q}) \simeq 2\mathcal{N}_{n,1D}^0 \frac{Dk_\parallel^2}{Dk_\parallel^2 + |\omega_m|}, \quad (27)$$

where $\mathcal{N}_{n,1D}^0$ is the 1D density of states at the Fermi energy in the normal metal and $D = l_e^2/\tau_e$ is the diffusion constant in 1D. The factor 2 accounts for the spin degeneracy.

In Fig. 3 we have plotted the dispersion relation $\omega(k_\parallel)$ vs $k_\parallel$ (thick solid line), obtained from numerical evaluation of Eq. (17), using the response function, Eq. (26), and the parameters of Table I, which correspond to typical experimen-

TABLE I. Parameters used in the calculations. Order-of-magnitude estimations of r_0 and L have been extracted from experiments on superconducting aluminum wires with coherence length estimated as $\xi_0 \sim 100$ nm (cf. Ref. 18).

$r_0 \simeq d$ (nm)	L (μm)	$\mathcal{D}_0$ ($\mathrm{kg}^{-1}\,\mathrm{m}^{-1}$)	$\mathcal{N}_{s,1D}^0 \simeq \mathcal{N}_{n,1D}^0$ ($\mathrm{m}^{-1}\,\mathrm{J}^{-1}$)	Δ_0 (K)	D ($\mathrm{m}^2\,\mathrm{s}^{-1}$)	ϵ_r	$w_{\rm film}$ (nm)	$k_{\rm TF}^{2D}$ (nm^{-1})	$\mathcal{N}_{n,2D}^0$ ($\mathrm{m}^2\,\mathrm{J}^{-1}$)
10	100	8.6×10^{35}	10^{29}	1	0.01	1	100	1	10^{38}

tal values.[18] Note that because of the diffusive pole at $\mathbf{q}=0$ in the response function $\chi^{(1)}_{0,n}(\mathbf{q})$ of the 1DEG [cf. Eq. (27)], the behavior of the 1D plasmon (and therefore the superconducting properties of the wire) will crucially depend on the way the limit $\mathbf{q}\to 0$ in Eq. (17) is taken. As is evident from the denominator in Eq. (27), the energy scale $|\omega_m|=Dk_\parallel^2$ separates two distinct regimes of screening. If the energy of the 1D plasmon is such that $\omega(k_\parallel)\simeq|\omega_m|\ll Dk_\parallel^2$, then the 1DEG response is essentially static, and consequently we call this the regime of "static" screening (light gray area in Fig. 3). Conversely, if $\omega(k_\parallel)\simeq|\omega_m|\gg Dk_\parallel^2$ (white area in Fig. 3), the dynamical response of the 1DEG dominates the screening, and therefore we refer to "dynamical" screening regime. In the next sections we study in detail the behavior of the 1D plasmon in these regimes.

1. Static screening limit $\omega(k_\parallel)\ll Dk_\parallel^2$

In this case, the response function in the normal metal [cf. Eq. (27)] can be Taylor expanded in powers of the small parameter $\frac{|\omega_m|}{Dk_\parallel^2}$. Truncating the series at first order, we obtain from Eq. (27) the expression $\chi^{(1)}_{0,n}(\mathbf{q})\simeq 2\mathcal{N}^0_n(1-\frac{|\omega_m|}{Dk_\parallel^2})$, and Eq. (17) reads

$$-\omega^2(k_\parallel)\left[1+i\frac{\alpha\omega(k_\parallel)}{Dk_\parallel^2}\right]+u^2k_\parallel^2=0, \tag{28}$$

where we have defined the velocity of the statically screened acoustic 1D plasmon,

$$u\equiv\sqrt{\frac{4\mathcal{D}_0}{\chi^{(1)}_s(0)}} \tag{29}$$

[compare to the momentum dependent $u(k_\parallel)$ in Eq. (21)]. $\alpha\equiv\frac{\chi_{0,s}(0)}{\chi_{0,s}(0)+2\mathcal{N}^0_{n,1D}}$ is a dimensionless parameter quantifying the amount of dissipation induced by the coupling to the diffusive 1DEG. Indeed, note that in the limit $\alpha\to 0$, Eq. (28) reproduces the linear dispersion relation of a 1D plasmon with infinite lifetime, which corresponds to the normal mode of a Luttinger-liquid action with short-range interactions[11] (note that in this case, the screening length for the Coulomb interactions is given by the distance d to the 1DEG). In the more general case, the term $\sim i\frac{\alpha\omega(k_\parallel)}{Dk_\parallel^2}$ in Eq. (28) introduces a small deviation from linearity, and more importantly, broadening in the plasmon mode [i.e., imaginary part in $\omega(k_\parallel)$].

In Fig. 4 we show the real and imaginary parts of $\omega(k_\parallel)$ as a function of $k_\parallel$, evaluated numerically directly from Eq. (17) and for the parameters of Table I. The curve $\omega=Dk_\parallel^2$ is shown as a reference. Note that while $\mathrm{Re}[\omega(k_\parallel)]$ follows an approximately linear dispersion relation in the regime $\omega(k_\parallel)<Dk_\parallel^2$, the imaginary part takes a constant value (meaning that the plasmon mode acquires a finite width). This result can be seen from Eq. (28) in the perturbative limit $\alpha\to 0$, where

$$\Gamma(k_\parallel)\equiv-\mathrm{Im}[\omega(k_\parallel)]\simeq\frac{\alpha u^2}{2D}. \tag{30}$$

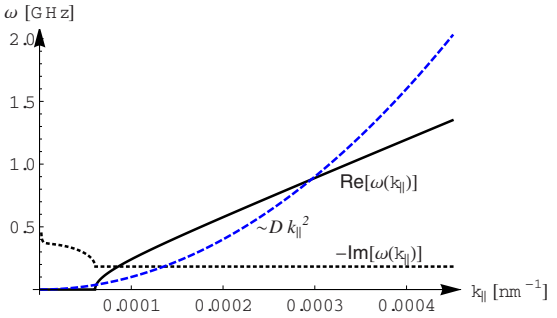

FIG. 4. (Color online) Real (solid line) and imaginary (dotted line) components of the 1D plasma mode $\omega(k_\parallel)$, obtained by numerical evaluation of the equation of motion Eq. (17), using Eq. (26). The real part (solid line) gives the dispersion relation while the imaginary part (dotted line) represents the damping of the mode. As in Fig. 3, the curves have been calculated for realistic experimental parameters (cf. Table I). The curve $\omega=Dk_\parallel^2$ (dashed line), indicating the crossover between the static and dynamical screening regimes, is shown as a reference.

2. Dynamical screening limit $\omega(k_\parallel)\gg Dk_\parallel^2$

Note that while the 1D plasmon follows an approximately linear dispersion relation $\sim uk_\parallel$ [cf. Eq. (28)], the crossover between the different regimes is $\sim Dk_\parallel^2$ [cf. Eq. (27)]. This qualitative argument indicates that in the limit $k_\parallel\to 0$, dynamical screening will eventually dominate. For realistic estimates of the experimental parameters (cf. Table I), our results indicate that the regime $\omega(k_\parallel)\gg Dk_\parallel^2$ (white area in Fig. 3) should be the most relevant in experimental studies on today's accessible wires.[16–18]

We note that if the condition

$$Dk_\parallel^2\ll|\omega_m|\ll\frac{2e^2}{\epsilon_r}\mathcal{N}^0_{n,1D}Dk_\parallel^2\ln\left(\frac{2}{k_\parallel r_0}\right), \tag{31}$$

is fulfilled, then the response function, Eq. (26), can be approximated as

$$\chi^{(1)}_s(\mathbf{q})\simeq 2\mathcal{N}^0_{n,1D}\frac{Dk_\parallel^2}{|\omega_m|}.$$

This results indicates that in this regime $\chi^{(1)}_s(\mathbf{q})\simeq\chi^{(1)}_n(\mathbf{q})$ [cf. Eq. (27)], which physically means that the superconductor "inherits" the diffusive dynamics in the 1DEG through the effect of the Coulomb interaction.

It is interesting to study the consequences on the action, Eq. (13), in this regime,

$$S^{\mathrm{w}}_{(1)}\simeq\frac{1}{2\beta L}\sum_{\mathbf{q}}\left[\frac{1}{2}\mathcal{N}^0_{n,1D}Dk_\parallel^2|\omega_m|+\mathcal{D}_0k_\parallel^2\right]|\theta(\mathbf{q})|^2. \tag{32}$$

In this effective action, phase fluctuations show dissipative dynamics (encoded in the term $\sim k_\parallel^2|\omega_m|$) as a consequence of the coupling to the dissipative processes in the 1DEG.

Note that a term $\sim k_\parallel^2|\omega_m|$ has been studied in the context of resistively shunted Josephson junctions arrays.[14,45,46] In that case, the term $\sim k_\parallel^2|\omega_m|$ appears *in addition* to the dynamical term $\sim\omega_m^2$, which represents the effect of quantum fluctuations induced by the charging energy of the supercon-

ducting island.[47] As a result, dissipation turns out to be beneficial to superconductivity, through the quenching of phase fluctuations.[45]

However, in our case, the form of the action in Eq. (32) is qualitatively different since the term $\sim\omega_m^2$ is *absent* (actually, it is the dynamical term *itself* which becomes a contribution $\sim k_\parallel^2|\omega_m|$). This has *detrimental* consequences for the superconductivity in the wire, as can be seen directly from the equation of motion for the field θ, Eq. (17), which gives $\omega(k_\parallel)\simeq -i2\mathcal{D}_0/(D\mathcal{N}^0_{n,1\mathrm{D}})$, indicating that the original plasma mode is completely damped (i.e., purely imaginary contribution) and vanishes in the limit $k_\parallel\to 0$ (see Fig. 3). Indeed, expressing the action, Eq. (32), in terms of the dual plasmon field[11] $\phi(\mathbf{x})$, defined as

$$\delta\rho_s(\mathbf{x}) \equiv -\frac{1}{\pi}\nabla\,\phi(\mathbf{x}), \tag{33}$$

we obtain the equivalent description,

$$S^{\mathrm{w}}_{(1)} \simeq \frac{1}{2\pi^2}\frac{1}{\beta L}\sum_{\mathbf{q}}\left[\frac{|\omega_m|}{2\mathcal{N}^0_{n,1\mathrm{D}}D}+\frac{\omega_m^2}{4\mathcal{D}_0}\right]|\phi(\mathbf{q})|^2,$$

which shows that the term $\sim k_\parallel^2|\omega_m|$ in Eq. (32) translates into a relevant term $\sim|\omega_m|$ (in the RG sense) when expressed in terms of the plasmon field $\phi(\mathbf{q})$. Another way to see this detrimental effect is through the order-parameter correlation function $F(\mathbf{x})$ [cf. Eq. (22)], which vanishes due to the infrared divergence of the phase correlator for $\tau>0$, i.e., $\langle T_\tau[\theta(x,\tau)-\theta(0)]^2\rangle \equiv \frac{2}{\beta L}\Sigma_{\mathbf{q}}\frac{1-\cos k_\parallel x+\omega_m\tau}{2\mathcal{N}^0_{n,1\mathrm{D}}Dk_\parallel^2|\omega_m|+\mathcal{D}_0k_\parallel^2}\to\infty$. For the particular case $\tau=0$, the space-dependent correlator reads

$$\langle T_\tau[\theta(x,0)-\theta(0)]^2\rangle \sim C\frac{|x|}{\mathcal{N}^0_{n,1\mathrm{D}}D}, \tag{34}$$

where $C\equiv -\frac{1}{4\pi}\exp[\frac{\mathcal{D}_0\tau_0}{2\mathcal{N}^0_{n,1\mathrm{D}}D}]\,\mathrm{Ei}(-\frac{\mathcal{D}_0\tau_0}{2\mathcal{N}^0_{n,1\mathrm{D}}D})$ [with $\mathrm{Ei}(z)$ the exponential-integral function[34]], meaning that the correlation function decreases exponentially fast with distance $F(x)\simeq\Delta_0^2\exp[-\frac{C|x|}{\mathcal{N}^0_{n,1\mathrm{D}}D}]$.

Only in the regime,

$$\frac{2e^2}{\epsilon_{\mathrm{r}}}\mathcal{N}^0_n Dk_\parallel^2\,\ln\frac{2}{k_\parallel r_0} \ll |\omega_m| \tag{35}$$

(cf. dark gray area and inset of Fig. 3), and provided Eq. (27) is still valid, or in the limit of very low electronic density of states in the 1DEG, we recover Eq. (21) describing again an unscreened 1D plasma mode.[10] Physically, at such high frequencies the response $\chi^{(1)}_{0,n}(\mathbf{q})$ of the 1DEG vanishes and the superconducting wire is effectively unscreened.

C. Screening by a diffusive metallic film

Now we focus our attention on the system of Fig. 1(b), which represents a superconducting wire coupled to a normal diffusive film of width w_{film}. In this case, the presence of the superconducting wire breaks the translational symmetry in the direction perpendicular to the wire. Consequently, the perpendicular momentum $k_\perp$ in the plane is not conserved and the Coulomb interaction [compare to Eq. (15)],

$$v^{(2)}(k_\parallel,k_\perp,d)=\frac{2\pi e^2}{\epsilon_{\mathrm{r}}}\frac{e^{-\sqrt{k_\parallel^2+k_\perp^2}d}}{\sqrt{k_\parallel^2+k_\perp^2}} \tag{36}$$

couples the density modes in the wire $\rho_s(\mathbf{q})$ with momentum $k_\parallel$ to all the modes in the plane $\rho_n(\mathbf{q},k_\perp)$ with momentum $k_\perp$.

In this case, the response function in the normal metal at low energies writes[44]

$$\chi^{(2)}_{0,n}(\mathbf{q},k_\perp)\simeq 2\mathcal{N}^0_{n,2\mathrm{D}}\frac{D(k_\parallel^2+k_\perp^2)}{D(k_\parallel^2+k_\perp^2)+|\omega_m|}, \tag{37}$$

where $\mathcal{N}^0_{n,2\mathrm{D}}$ is the 2D density of states at the Fermi energy in the normal metal. Here again, we neglect Anderson-localization effects in the metal by assuming that the length of the wire is $L\ll\xi_{\mathrm{film}}$, where ξ_{film} is the localization length in the film.

We concentrate on the effective 1D potential $v^{(2)}_{\mathrm{eff}}(\mathbf{q})$ encoding the screening properties of the diffusive film is [cf. Eq. (16)]

$$v^{(2)}_{\mathrm{eff}}(\mathbf{q}) \equiv \frac{1}{L_\perp}\sum_{k_\perp}\frac{[v^{(2)}(k_\parallel,k_\perp,d)]^2\chi^{(2)}_{0,n}(\mathbf{q},k_\perp)}{1+v^{(2)}(k_\parallel,k_\perp,0)\chi^{(2)}_{0,n}(\mathbf{q},k_\perp)}$$

$$=\frac{2e^2}{\epsilon_{\mathrm{r}}}\frac{Dk_{\mathrm{TF}}}{2}\int dk_\perp e^{-2\sqrt{k_\parallel^2+k_\perp^2}d}$$

$$\times\frac{1}{D(k_\parallel^2+k_\perp^2)+Dk_{\mathrm{TF}}\sqrt{k_\parallel^2+k_\perp^2}+|\omega_m|}, \tag{38}$$

where we have defined the 2D Thomas-Fermi wave vector,

$$k_{\mathrm{TF}}\equiv\frac{4\pi e^2\mathcal{N}^0_{n,2\mathrm{D}}}{\epsilon_{\mathrm{r}}}.$$

This quantity defines the 2D Thomas-Fermi screening length $\lambda^{2\mathrm{D}}_{\mathrm{TF}}=\frac{2\pi}{k_{\mathrm{TF}}}$, beyond which the Coulomb potential is completely screened.[32]

As in Sec. III B, the way in which the limit $\mathbf{q}\to 0$ is taken in Eq. (38) determines the screening regime provided by the 2DEG, and the behavior of the 1D plasmon. Again, two distinct regimes appear, although in this case the 1D plasmon energy $\omega(k_\parallel)$ is to be compared to the energy scale $Dk_{\mathrm{TF}}|k_\parallel|$ (rather than $Dk_\parallel^2$) as is evident from the denominator in Eq. (38). The case $\omega(k_\parallel)\ll Dk_{\mathrm{TF}}|k_\parallel|$ corresponds to the static screening regime while $\omega(k_\parallel)\gg Dk_{\mathrm{TF}}|k_\parallel|$ is the dynamical screening regime.

1. Static screening limit $\omega(k_\parallel)\ll Dk_{\mathrm{TF}}|k_\parallel|$

This region corresponds to the gray area in Fig. 5. In this regime, the integrand of the effective potential $v^{(2)}_{\mathrm{eff}}(\mathbf{q})$, Eq. (38), can be Taylor expanded in powers of $|\omega_m|/[D(k_\parallel^2+k_\perp^2)+Dk_{\mathrm{TF}}\sqrt{k_\parallel^2+k_\perp^2}]$, and in the experimentally relevant limit $k_{\mathrm{TF}}d\gg 1$, this expression reduces to

$$v^{(2)}_{\mathrm{eff}}(\mathbf{q})\simeq\frac{2e^2}{\epsilon_{\mathrm{r}}}\left[K_0(2k_\parallel d)-\frac{\pi}{2}\frac{|\omega_m|}{Dk_{\mathrm{TF}}|k_\parallel|}\right] \tag{39}$$

with $K_0(z)$ the zeroth-order modified Bessel function.[34] When replaced into Eq. (13), the effective potential, Eq. (39),

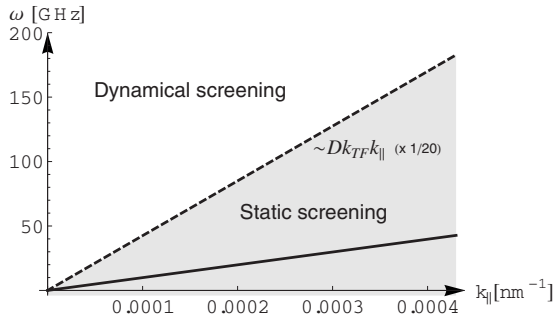

FIG. 5. Screening regimes for a superconducting wire capacitively coupled to a diffusive 2DEG. The dispersion relation (solid line) results from Eq. (41), valid in the regime $\omega(k_\parallel) \ll Dk_{\rm TF}|k_\parallel|$. The dashed line $\omega = Dk_{\rm TF}|k_\parallel|$ separates the regime of static (light gray area) from that of dynamic (white area) screening. The parameters used in the calculations are shown in Table I.

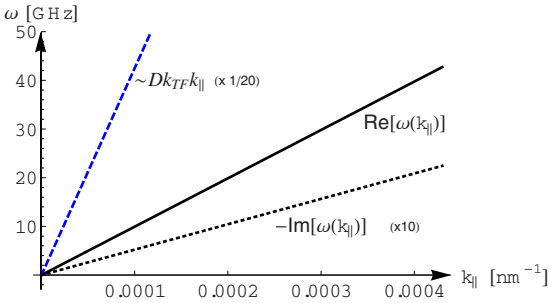

FIG. 6. (Color online) Real and imaginary components of the 1D plasma mode $\omega(k_\parallel)$, obtained by numerical evaluation of the equation of motion Eq. (41), valid in the regime $\omega(k_\parallel) \ll Dk_{\rm TF}|k_\parallel|$. The blue dashed line $\omega = Dk_{\rm TF}k_\parallel$ separates the regime of static (light gray area) from that of dynamic (white area) screening. The parameters used in the calculations are in Table I.

contributes a term $\sim|\omega_m|^3/k_\parallel$ (which is marginally relevant in the RG sense) to the effective action, and has the effect of renormalizing the bare parameters in a Luttinger-liquid description.[48] The first and second terms in Eq. (39) are, respectively, consistent with the static and dissipative contributions to the effective screened interaction, obtained for a Tomonaga-Luttinger liquid electrostatically coupled to a diffusive 2DEG (cf. Ref. 24). The static screening provided by the 2DEG [first term in Eq. (39)] cuts the logarithmic divergence of the bare intrawire Coulomb interaction $v^{(1)}(k_\parallel,0)$ in Eq. (15). The relation between the second term in Eq. (39) and the dissipative contribution $\sim k_\parallel|\omega_m|$ in Ref. 24 can be made explicit with the introduction of the plasmon field $\phi(\mathbf{x})$, defined in Eq. (33).

In the limit $k_\parallel \to 0$ [with $\omega(k_\parallel) \ll Dk_{\rm TF}|k_\parallel|$], the form of the effective potential, Eq. (39), can be further simplified to $v^{(2)}_{\rm eff}(\mathbf{q}) \simeq \frac{2e^2}{\epsilon_r}[\ln(\frac{1}{k_\parallel d}) - \frac{\pi}{2}\frac{|\omega_m|}{Dk_{\rm TF}|k_\parallel|}]$, and when replaced in Eq. (14) yields

$$\chi_s^{(2)}(\mathbf{q}) \simeq \frac{\chi_{0,s}(0)}{1+\chi_{0,s}(0)\dfrac{2e^2}{\epsilon_{\rm r}}\left[\ln\left(\dfrac{2d}{r_0}\right)+\dfrac{\pi}{2}\dfrac{|\omega_m|}{Dk_{\rm TF}|k_\parallel|}\right]}. \quad (40)$$

From Eq. (17) we obtain the equation of motion for the 1D plasmon,

$$-\omega^2(k_\parallel) + i\frac{2e^2}{\epsilon_{\rm r}}\frac{2\pi\chi_s^{(2)}(0)}{Dk_{\rm TF}}\frac{\omega^3(k_\parallel)}{|k_\parallel|} + u^2k_\parallel^2 = 0, \quad (41)$$

where

$$u = \sqrt{\frac{4\mathcal{D}_0}{\chi_s^{(2)}(0)}}$$

is the velocity of the statically screened plasmon [note the similarity with Eq. (29)]. Equation (41) describes a 1D plasma mode with approximately linear dispersion relation and width,

$$\Gamma(k_\parallel) = -\,{\rm Im}[\omega(k_\parallel)] \sim \frac{\pi e^2\mathcal{D}_0}{2\epsilon_{\rm r}Dk_{\rm TF}\chi_{s,0}(0)}|k_\parallel|. \quad (42)$$

In Fig. 5 we show (solid line) the dispersion relation obtained from Eq. (41) [i.e., real component of $\omega(k_\parallel)$] for the parameters in Table I. The light-gray area represents the regime of static screening (note that we have multiplied the curve $\omega = Dk_{\rm TF}|k_\parallel|$ by a factor $\frac{1}{20}$ in order to visualize better our results). For the parameters of Table I, the estimated plasmon velocity is $u \sim 10^5$ m s$^{-1} \ll Dk_{\rm TF} \sim 10^7$ m s^{-1}, which indicates that the static screening regime is the most relevant one in the limit $k_\parallel \to 0$. For completeness, in Fig. 6 we show both the real and imaginary components of $\omega(k_\parallel)$. From Eq. (42), we obtain that the width of the plasmon depends linearly on $|k_\parallel|$.

Note that in the limit $D \to \infty$ (no dissipation in the normal metallic film), the solution of Eq. (41) corresponds to an infinitely long-lived plasma mode with linear dispersion relation.[11] Accordingly, Eq. (13) reduces to the action of a Tomonaga-Luttinger liquid with short-range interactions.[11]

2. Dynamical screening limit $\omega(k_\parallel) \gg Dk_{\rm TF}|k_\parallel|$

If the screening properties of the 2DEG are poor (i.e., low values of the electronic density and diffusion constant), it may occur that the condition of static screening $\omega(k_\parallel) \ll Dk_{\rm TF}|k_\parallel|$ is not fulfilled, and consequently the approximation, Eq. (39), does not apply. We therefore need to explore the regime of plasmon frequencies $\omega(k_\parallel) \gg Dk_{\rm TF}|k_\parallel|$. In this regime (white area in Fig. 5), the effective potential $v^{(2)}_{\rm eff}(\mathbf{q})$ in Eq. (38) can be approximated as

$$v^{(2)}_{\rm eff}(\mathbf{q}) \approx \frac{2e^2}{\epsilon_{\rm r}}\left[f(2k_{\rm TF}d) - f\left(\frac{2|\omega_m|d}{Dk_{\rm TF}}\right)\right],$$

where we have defined $f(z) \equiv -e^z\,{\rm Ei}(-z)$ with ${\rm Ei}(x)$ the exponential-integral function.[34] If the additional condition $|\omega_m| \ll \frac{Dk_{\rm TF}}{d}$ holds, the effective potential can be further simplified to

$$v_{\mathrm{eff}}^{(2)}(\mathbf{q}) \simeq \frac{2e^2}{\epsilon_r}\ln\left(\frac{2d|\omega_m|}{Dk_{\mathrm{TF}}}\right). \tag{43}$$

Using this expression, the response function, Eq. (14), reads

$$\chi_s^{(2)}(\mathbf{q}) \simeq \frac{\chi_{0,s}(0)}{1+\frac{2e^2}{\epsilon_r}\chi_{0,s}(0)\ln\left(\frac{Dk_{\mathrm{TF}}}{dr_0k_\parallel|\omega_m|}\right)}, \tag{44}$$

which results in the equation of motion obtained from Eq. (17) (in the limit $\mathbf{q}\to 0$),

$$-\omega(k_\parallel)^2 + u_0^2k_\parallel^2\left(\ln\left|\frac{Dk_{\mathrm{TF}}}{dr_0k_\parallel\omega(k_\parallel)}\right| + i\frac{\pi}{2}\right) = 0 \tag{45}$$

with u_0 defined in Eq. (25). As in the unscreened case of Sec. III A, the presence of the logarithm is an indication that the 2DEG fails to screen completely the Coulomb interaction. Contrarily to the case studied in Sec. III B, the resulting plasma mode is not damped in the limit $k_\parallel\to 0$, i.e., a dispersive real component survives. From Eq. (45) it is possible to show that in the limit $k_\parallel\to 0$,

$$\mathrm{Re}[\omega(k_\parallel)] \simeq u_0k_\parallel\sqrt{\ln\left|\frac{Dk_{\mathrm{TF}}}{dr_0u_0k_\parallel^2}\right|}, \tag{46}$$

$$\mathrm{Im}[\omega(k_\parallel)] \simeq -\frac{\pi}{4}\frac{u_0k_\parallel}{\sqrt{\ln\left|\frac{Dk_{\mathrm{TF}}}{dr_0u_0k_\parallel^2}\right|}}, \tag{47}$$

meaning that the width of the 1D plasma mode decreases at low energies, resulting again in a well-defined excitation. Note the difference with respect to the screening provided by a 1DEG, where the damping of the plasmon is complete in the limit $k_\parallel\to 0$. The origin of this difference lies in the additional degree of freedom $k_\perp$ (momentum perpendicular to the wire), which smears (upon integration) the dependence on the damping factor $|\omega_m|$ in the susceptibility [cf. Eq. (38)].

In the regime of frequencies $\frac{Dk_{\mathrm{TF}}}{d} \ll |\omega_m| \ll Dk_{\mathrm{TF}}^2$, the effective potential $v_{\mathrm{eff}}^{(2)}(\mathbf{q})$ can be approximated as

$$v_{\mathrm{eff}}^{(2)}(\mathbf{q}) \approx \frac{2e^2}{\epsilon_r}\frac{1}{2k_{\mathrm{TF}}d}\left[1-\frac{Dk_{\mathrm{TF}}^2}{|\omega_m|}\right]$$

and the response function is

$$\chi_{0,s}^{(2)}(\mathbf{q}) \simeq \frac{\chi_{0,s}(0)}{1+\frac{2e^2}{\epsilon_r}\chi_{0,s}(0)\left[\ln\left(\frac{2}{k_\parallel r_0}\right)+\frac{Dk_{\mathrm{TF}}}{2d|\omega_m|}\right]}. \tag{48}$$

In this limit, the equation of motion of the field $\theta(\mathbf{q})$ is

$$-\omega^2(k_\parallel) + u_0^2k_\parallel^2\left[\ln\left(\frac{2}{k_\parallel r_0}\right)+\frac{iDk_{\mathrm{TF}}}{2d\omega(k_\parallel)}\right] = 0.$$

Note that in this regime, the dissipative effects are weaker and the dispersion relation resembles that of the (unscreened) Mooij-Schön mode, Eq. (21). Eventually in the limit $|\omega_m| \gg Dk_{\mathrm{TF}}^2$, the response $\chi_{0,n}^{(2)}(\mathbf{q})$ of the 2DEG vanishes and the wire is effectively in the unscreened regime where the Mooij-Schön plasma mode of Eq. (21) is fully recovered. However, for the parameters of Table I and in the limit $k_\parallel\to 0$, we have not found solutions consistent with the condition $\omega(k_\parallel) \gg Dk_{\mathrm{TF}}k_\parallel$, and therefore conclude that only the static screening regime is relevant.

IV. DISSIPATIVE EFFECTS IN THE DYNAMIC CONDUCTIVITY

In this section we study the consequences of the dissipative effects on the dynamic conductivity of the wire $\sigma(k_\parallel,\omega)$, i.e., the ratio between the current density and the local electric field $j(k_\parallel,\omega)=\sigma(k_\parallel,\omega)E(k_\parallel,\omega)$. This quantity is of interest because its real part $\mathrm{Re}[\sigma(k_\parallel,\omega)]$ provides information on the absorption properties and dissipation, which results from the coupling to the diffusive modes in the electron gas.[49]

The response of the system to an external electromagnetic field can be obtained by the means of the minimal coupling $-i\nabla\to -i\nabla-\frac{e}{c}A$ in the microscopic Hamiltonian (3). For a superconducting wire at $T=0$ and in absence of quasiparticle excitations, the total current density is given by

$$j(\mathbf{x}) = j_p(\mathbf{x}) + j_d(\mathbf{x}),.$$

$$j_p(\mathbf{x}) = \frac{2e}{c}\mathcal{D}_0\nabla\,\theta(\mathbf{x}),$$

$$j_d(\mathbf{x}) = -\left(\frac{2e}{c}\right)^2\mathcal{D}_0A(\mathbf{x}),$$

where j_p and j_d are, respectively, the paramagnetic and diamagnetic contributions to the current density. The linear response to an applied electromagnetic field is given by the current-current susceptibility of the wire,

$$\chi_{jj}(\mathbf{q}) = \left.\frac{\delta\ln Z}{\delta A_{\mathbf{q}}\delta A_{-\mathbf{q}}}\right|_{A=0} = \langle j_p(\mathbf{q})j_p(-\mathbf{q})\rangle - \mathcal{D}_0\left(\frac{2e}{c}\right)^2.$$

Defining the quantity $\sigma(\mathbf{q})=-\frac{\chi_{jj}(\mathbf{q})}{\omega_m}$, the conductivity is obtained upon analytical continuation to real frequencies[11,32] $\sigma(k_\parallel,\omega)=\sigma(\mathbf{q})|_{i\omega_m\to\omega+i\delta}$. In terms of the phase field $\theta(\mathbf{q})$, the conductivity reads

$$\sigma(\mathbf{q}) \equiv -\left(\frac{2e}{c}\right)^2\left[-\frac{\mathcal{D}_0}{\omega_m}+\frac{\mathcal{D}_0^2k_\parallel^2}{\omega_m}\langle\theta(\mathbf{q})\theta(-\mathbf{q})\rangle\right]. \tag{49}$$

Let us first study the response of an ideally isolated wire (cf. Sec. III A) to the electromagnetic field. At $T=0$ we obtain

$$\mathrm{Re}[\sigma(k_\parallel,\omega)] = \frac{\pi}{2}\mathcal{D}_0\left(\frac{2e}{c}\right)^2\delta[\omega-\omega(k_\parallel)], \tag{50}$$

where $\omega(k_\parallel)=\sqrt{\frac{8e^2\mathcal{D}_0}{\epsilon_r}\ln(\frac{2}{|k_\parallel r_0|})k_\parallel^2}$ is the energy of the Mooij-Schön plasmon [cf. Eq. (21)]. The real part of the conductivity tells us that the system absorbs energy at the frequency $\omega=\omega(k_\parallel)$, which in this case are well-defined excitations (i.e., delta functions). Note that in the limit $k_\parallel\to 0$, Eq. (50) allows to recover the Drude peak at $\omega=0$, which is expected for a superconductor.[11,32]

Let us now consider the case of a wire in the proximity to a g-DEG. Using the action, Eq. (13), to evaluate the formula

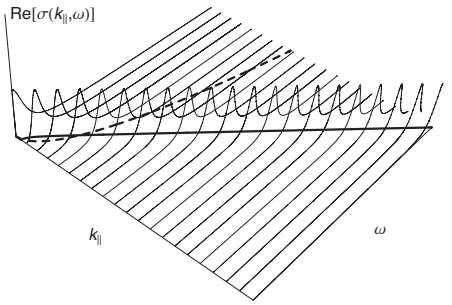

FIG. 7. Dynamic conductivity Re $\sigma(k_\parallel,\omega)$ of a superconducting wire dynamically screened by a diffusive 1DEG. The plasma mode, which is better defined at high energy and momentum becomes completely damped in the limit $\{\omega,k_\parallel\}\to 0$ by the effects of the dissipative environment.

of the conductivity, Eq. (49), we obtain the expression (valid at $T=0$)

$$\mathrm{Re}[\sigma(k_\parallel,\omega)] = \mathcal{D}_0^2\left(\frac{2e}{c}\right)^2\frac{k_\parallel^2}{\omega} \times \mathrm{Im}\left[k_\parallel^2\mathcal{D}_0 - \frac{(\omega+i0^+)^2}{4}\chi^{(g)}_{s,\mathrm{ret}}(k_\parallel,\omega)\right]^{-1}, \tag{51}$$

where $\chi^{(g)}_{s,\mathrm{ret}}(k_\parallel,\omega)\equiv \lim_{\delta\to 0^+}[\chi^{(g)}_s(\mathbf{q})]_{i\omega_m\to\omega+i\delta}$.

We first study the case of screening by a diffusive 1DEG (cf. Sec. III B 2), where the effects of dissipation are at their strongest. We concentrate here only on the experimentally relevant regime, Eq. (31), and do not consider the regime, Eq. (35), relevant, in principle, for much longer wires. In Fig. 7 we show the result for $\mathrm{Re}[\sigma(k_\parallel,\omega)]$ of Eq. (51) as a function of $k_\parallel$ and ω. In the bottom $(k_\parallel,\omega)$ plane, we show the dispersion relation $\mathrm{Re}[\omega(k_\parallel)]$ vs $k_\parallel$ (thick solid line), corresponding to the same plot of Fig. 3. As mentioned before, the absorption peaks of $\mathrm{Re}[\sigma(k_\parallel,\omega)]$ are centered at the frequency $\mathrm{Re}[\omega(k_\parallel)]$ of the plasma mode. The curve $Dk_\parallel^2$ (dashed line) is also plotted in the bottom $(k_\parallel,\omega)$ plane in order to visualize the different screening regimes. Note that the dissipative effects in the normal wire (encoded in a finite value of the diffusion constant D) are manifested in this figure through the finite width $\Gamma(k_\parallel)\simeq -\mathrm{Im}[\omega(k_\parallel)]$ of the plasmon peaks. Note in addition that the constant width $\Gamma(k_\parallel)$ in the regime $\omega(k_\parallel)\gg Dk_\parallel^2$ is consistent with the result for $\mathrm{Im}[\omega(k_\parallel)]$ of Fig. 4.

As $k_\parallel\to 0$, the plasmon peak merges smoothly into the dc-conductivity value $\sigma_{\mathrm{dc}}=(\frac{2e}{c})^2 2D\mathcal{N}^0_{n,1\mathrm{D}}$, which exactly corresponds to the dc conductivity of the 1DEG (cf. Fig. 8). Physically, this means that the dissipative processes in the 1DEG are transferred to the superconductor via the Coulomb interaction. It also indicates that the original plasma mode is no longer a well-defined excitation of the system, and that the electromagnetic environment has profound consequences in the excitation spectrum of the 1D superconductor.

As we mentioned before, far from the BKT quantum critical point, phase slips are an irrelevant perturbation (in the RG sense). In the case of Luttinger liquids with short-range

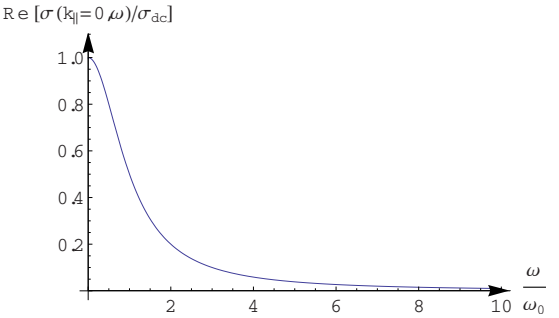

FIG. 8. (Color online) dc conductivity $\sigma(\omega)=\mathrm{Re}[\sigma(k_\parallel\to 0,\omega)]$ of a superconducting wire screened by a diffusive 1DEG. The values on the axis are normalized to $\sigma_{\mathrm{dc}}=\sigma(\omega=0)=(\frac{2e}{c})^2 2D\mathcal{N}^0_{n,1\mathrm{D}}$ and $\omega_0\equiv\frac{\mathcal{D}_0}{2\mathcal{N}^0_{n,1\mathrm{D}}D}$. The plasma mode is completely damped in the limit $k_\parallel\to 0$ (cf. Fig. 7) and the wire presents finite resistivity.

interactions, the perturbative effect of phase slips generates a power-law resistivity $\varrho\sim T^\nu$, with ν a positive exponent.[38] Although we have neglected the perturbative effect of topological excitations in our formalism, the fact that a finite resistivity at $T=0$ appears in the superconducting wire indicates that their effect in the conductivity might be negligible as compared to those induced by dissipation in the electron gas discussed here.

In the case of screening by a diffusive 2DEG, our main results are presented in Fig. 9. Contrarily to the case of Fig. 7, the plasmon peaks centered at $\mathrm{Re}[\omega(k_\parallel)]$ are better defined, and their width eventually vanish in the limit $k_\parallel\to 0$, in agreement with Eq. (42) and Fig. 6. Eventually, the plasmon peak merges into the superconducting Drude peak at $\omega=0$.

The presence of an additional degree of freedom (i.e., momentum $k_\perp$ in the plane perpendicular to the wire) is of central importance to understand the vanishing of dissipation. Indeed, even in the dynamical screening regime $|\omega_m|\gg Dk_{\mathrm{TF}}|k_\parallel|$ for which one would naively think that dissipation effects are dominant, the existence of a wave vector $k_\perp$ satisfying the condition $|\omega_m|\ll Dk_\perp^2$ makes the dissipative processes less important. Note in addition that this condition is

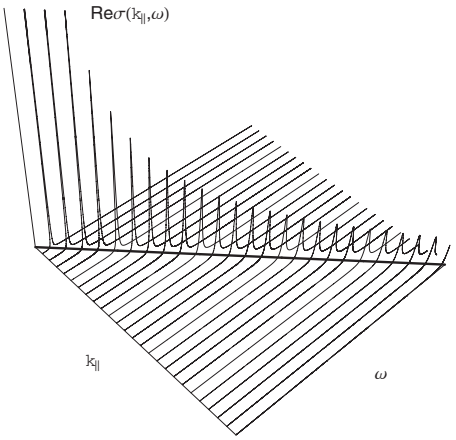

FIG. 9. Dynamic conductivity $\mathrm{Re}[\sigma(k_\parallel,\omega)]$ of a superconducting wire dynamically screened by a diffusive 2DEG. The plasma mode is worse defined at high energy and momentum but in the limit $\{\omega,k_\parallel\}\to 0$ the effects of dissipation vanish.

more easily satisfied in the limit $|\omega_m| \to 0$. These qualitative phase-space considerations allow to understand the behavior of the effective 1D potential $v_{\mathrm{eff}}^{(2)}(\mathbf{q})$ of Eq. (43), which has a weaker (i.e., logarithmic) dependence on the term $|\omega_m|$ encoding the dissipation. The net result is that the 1D plasma modes are better defined in the limit $k_\parallel \to 0$ and frictional effects vanish.

V. DISCUSSION AND SUMMARY

In this paper we have studied the effects of the local electromagnetic environment, provided by the presence of a noninteracting electron gas, on the low-energy physics of a superconducting wire. In particular, we have focused on the derivation of an effective phase-only action, starting from the microscopic Hamiltonian of the system. Using the path-integral formalism, we decouple the superconducting and Coulomb interactions by the means of Hubbard-Stratonovich fields, and expand the resulting action in terms of Gaussian fluctuations around the saddle point. This treatment is equivalent to performing the so-called RPA approximation of the interacting problem.[32] We have studied two particular cases, namely, the screening provided by (a) a diffusive 1DEG, and (b) a diffusive 2DEG, both placed at a distance $d \simeq r_0$ from the wire. This would be the relevant situation in practical realizations in, e.g., superconductor/normal heterostructures made by the means of the ferroelectric field effect in Nb-doped $SrTiO_3$ layers[50] or in electrically controlled $LaAlO_3/SrTiO_3$ interfaces.[51,52]

It is of interest to put our results in the context of other works dealing with electrostatically coupled 1D systems. Among these, the Coulomb drag effect,[53] where a finite current I_1 is driven in one (the "active") system, and a finite voltage V_2 is induced in the other ("passive" system), has received a great deal of attention both theoretically[54–58] and experimentally.[59–61] Rather than dealing with out-of-equilibrium transport properties, inherent to the Coulomb drag effect, here we have concentrated on equilibrium properties of the wire and on the behavior of the 1D plasma mode.

From the theoretical point of view, our work differs from the usual Tomonaga-Luttinger-liquid description of a purely 1D (i.e., one electronic conduction channel) conductor, where the main mechanism of momentum decay is backscattering.[24,56–58] Indeed, it is worth to note that backscattering effects are absent in clean wires with a large number of electronic channels, and this fact is correctly reproduced by our effective coarse-grained theory [cf. Eq. (13)]. Therefore, in the language of Tomonaga-Luttinger-liquid physics, our treatment amounts to retaining only forward-scattering processes.

Our results point toward a rich behavior of the 1D plasma mode in the wire, determined by the screening properties of the diffusive electron gas. Independently of its dimensionality, in the static screening limit, the plasmon follows approximately a linear dispersion relation. One could naively think that in that regime dissipative effects are always negligible. However, the complete solutions of Eqs. (28) and (41) indicate that this is not the case. Indeed, we obtain sizable dissipative effects even in the limit $\omega(k_\parallel) \ll D k_\parallel^2$, in the presence of a 1DEG [$\omega(k_\parallel) \ll D k_{\mathrm{TF}} k_\parallel$ for a 2DEG], which are manifest in the broadening of the 1D plasmon mode (cf. Figs. 7 and 9). We have derived Eqs. (30) and (42), which relate the width of the plasmon to the diffusive properties of the electron gas (i.e., the diffusion constant D). Although technically challenging from the experimental point of view, this broadening could be seen in experiments of resonant inelastic Raman light-scattering[62] or in optical measurements of the dynamical conductivity or the reflection coefficient.[63]

On the other hand, our results indicate that in the dynamical regime, the dimensionality of the electron gas is of central importance to determine the behavior of the 1D plasmon, and determines the superconducting properties at low energy. If the screening is provided by a 1DEG, its dissipative processes are more efficiently transferred to the superconducting wire in the limit $k_\parallel \to 0$. As a consequence, the plasma mode becomes an ill-defined excitation and the superconductor shows a finite dc conductivity in the limit $\omega = 0$ (cf. Figs. 7 and 8). This effect could be seen, e.g., in dc-transport experiments on capacitively coupled superconducting/normal wires systems (cf. Fig. 8). More importantly, our results indicate that in the case of proximity to a 1DEG, the dynamical screening regime, Eq. (31), should be the most relevant for experimental realizations (cf. Figs. 3 and 5). This is more or less evident from the fact that the plasma mode essentially follows a linear dispersion in the limit $k_\parallel \to 0$ while the boundary between the dynamical and the static screening regimes (determined by the diffusive modes in the electron gas) is $\sim D k_\parallel^2$.

When the screening is provided by a 2DEG, acoustic plasma modes with a vanishing width are recovered in the limit $k_\parallel \to 0$. The reason for this lies in the existence of the additional degree of freedom in the electron gas (perpendicular momentum $k_\perp$), which produces (upon integration) a weakening of dissipation effects. At this point it is tempting to speculate that a semi-infinite three-dimensional (3D) metal, or a superconducting wire embedded in a 3D normal matrix, would provide an additional degree of freedom (momentum $k'_\perp$ perpendicular to $k_\parallel$ and $k_\perp$), and would weaken further the impact of dissipation in the metal.

These remarks are relevant to works suggesting the possibility to stabilize the superconductivity in 1D systems by coupling them to a bath of normal quasiparticles.[13,25,26] In these works, the basic underlying physical idea is that the normal bath provides a source of friction for the phase field $\theta(\mathbf{x})$ which tends to quench its fluctuations and therefore, to favor superconductivity (very much like in the case of a resistively shunted Josephson junction[2–4]). However, little attention has been given up to now to the simultaneous dissipative effects induced by the Coulomb interaction with the electrons in the metal, which produce friction in the dual field $\delta\rho_s(\mathbf{x})$, and therefore tends to increase phase fluctuations, deteriorating the superconducting properties. In that sense, our results show that the best condition would be to screen the Coulomb interaction with a clean (i.e., large diffusion constant D) metallic film (rather than a wire). This result lends credence to the analysis made in Ref. 26, where it was assumed that the Coulomb interactions only renormalize the bare Luttinger parameters of a superconducting wire

in contact with a 2D normal diffusive metal system.

Many other issues remain to be addressed to get an accurate physical description of a superconducting wire coupled to a dissipative electron gas, such as the aforementioned effect of topological excitations,[12] Anderson localization effects in the electron gas as a consequence of disorder, simultaneous effect of Coulomb interactions and Andreev tunneling, etc. We expect that our results inspire other works along these lines.

ACKNOWLEDGMENTS

This work was supported by the Swiss National Foundation under MaNEP and division II. A.M.L. acknowledges useful discussions with M. A. Cazalilla.

APPENDIX A: DERIVATION OF THE EFFECTIVE ACTION

Although the derivation of the low-energy action for a superconductor has been studied by several authors,[12,21,29,30] here we follow more closely the derivation of De Palo *et al.*[21] Our starting point is the decoupling of the interaction terms appearing in H_s^0 and $H_{\rm int}$ [Eqs. (3) and (8), respectively] by the means of HS transformations (HSTs),

$$e^{-\int d\tau H_{\rm int}(\tau)} \propto \int \prod_{\nu} \mathcal{D}[\tilde{\rho}_\nu] e^{-(1/2)\sum_{\nu=\pm}\int d^4x_\mu d^4x'_\mu [v_\nu(x_\mu - x'_\mu)]^{-1} \times \tilde{\rho}_\nu(x_\mu)\tilde{\rho}_\nu(x'_\mu) + i\int d^4x_\mu \hat{\rho}_\nu(x_\mu)\tilde{\rho}_\nu(x_\mu)}, \tag{A1}$$

$$e^{|U|\int d\mathbf{r}d\tau \psi^*_{s,\uparrow}\psi^*_{s,\downarrow}\psi_{s,\downarrow}\psi_{s,\uparrow}} \propto \int \mathcal{D}[\Delta^*,\Delta] e^{-\int d^4x_\mu (|\Delta(x_\mu)|^2/|U|) + \int d^4x_\mu \Delta^*(x_\mu)\psi_{s,\downarrow}(x_\mu)\psi_{s,\uparrow}(x_\mu) + \psi^*_{s,\uparrow}(x_\mu)\psi^*_{s,\downarrow}(x_\mu)\Delta(x_\mu)}, \tag{A2}$$

where we have introduced the notation $x_\mu=(\mathbf{r},\tau)$ and the bosonic fields $\tilde{\rho}_\nu(x_\mu)$, $\Delta^*(x_\mu)$, $\Delta(x_\mu)$. The quantity $[v_\nu(x_\mu - x'_\mu)]^{-1}$ is a compact notation for the Fourier transform,

$$[v_\nu(x_\mu - x'_\mu)]^{-1} = \frac{1}{\beta\Omega}\sum_{k^\mu} \frac{e^{ik^\mu(x_\mu - x'_\mu)}}{v_\nu(k^\mu)}, \tag{A3}$$

where $v_\nu(k^\mu)=\int d^4x_\mu e^{-ik^\mu(x_\mu - x'_\mu)} v_\nu(x_\mu - x'_\mu)$ with $v_\nu(x_\mu - x'_\mu)$ the potential $v_\nu(x_\mu - x'_\mu) \equiv v_\nu(\mathbf{r}-\mathbf{r}')\delta(\tau-\tau')$. Note that the mode $k^\mu=0$, for which the above HST is formally ill defined, can be safely ignored by considering the interaction with the positive ionic background in the system (not explicitly written here).

Our next step is to decouple the quadratic term $\tilde{\rho}_\nu(x_\mu)\tilde{\rho}_\nu(x_{\mu'})$ in Eq. (A1) by the means of an extra HST. According to Ref. 21, this has the advantage of introducing the *physical densities* (symmetric and antisymmetric) of the problem [cf. Eq. (7)]. Then,

$$e^{-(1/2)\int d^4x_\mu d^4x'_\mu [v_\nu(x_\mu - x'_\mu)]^{-1}\tilde{\rho}_\nu(x_\mu)\tilde{\rho}_\nu(x'_\mu)} \propto \int \mathcal{D}[\rho_\nu] e^{-(1/2)\int d^4x_\mu d^4x'_\mu \rho_\nu(x_\mu)v_\nu(x_\mu - x'_\mu)\rho_\nu(x'_\mu) - i\int d^4x_\mu \tilde{\rho}_\nu(x_\mu)\rho_\nu(x_\mu)}. \tag{A4}$$

Note that the formal integration of the field $\tilde{\rho}_\nu$ gives the functional-delta function[31] $\delta[\hat{\rho}_\nu - \rho_\nu]$. This fact allows to interpret the HS fields ρ_ν as the physical electronic densities.[21]

It is convenient to write the action of the system after these manipulations,

$$\begin{aligned} S = &\int d^4x_\mu \sum_\sigma \left\{ \psi^*_{s,\sigma}(\partial_\tau - \mu_s)\psi_{s,\sigma} + \frac{1}{2m}[\nabla\psi^*_{s,\sigma}][\nabla\psi_{s,\sigma}] \right\} \\ &+ \int d^4x_\mu \left\{ \frac{|\Delta(x_\mu)|^2}{|U|} - \Delta^*(x_\mu)\psi_{s,\downarrow}\psi_{s,\uparrow} - \psi^*_{s,\uparrow}\psi^*_{s,\downarrow}\Delta(x_\mu) \right\} \\ &+ \int dx_\mu \sum_\sigma \left\{ \psi^*_{n,\sigma}(\partial_\tau - \mu_n + V_{\rm i})\psi_{n,\sigma} + \frac{1}{2m}[\nabla\psi^*_{n,\sigma}] \times [\nabla\psi_{n,\sigma}] \right\} + \frac{1}{2}\sum_{\nu=\pm}\int d^4x_\mu d^4x'_\mu \rho_\nu(x_\mu)v_\nu(x_\mu - x'_\mu)\rho_\nu(x'_\mu) \\ &+ i\sum_{\nu=\pm}\int d^4x_\mu \tilde{\rho}_\nu(x_\mu)[\rho_\nu(x_\mu) - \hat{\rho}_\nu(x_\mu)], \end{aligned} \tag{A5}$$

where for simplicity we have dropped the arguments in the fermionic fields $\psi_{s,\sigma}$ and $\psi_{n,\sigma}$ and in the disorder potential $V_i=V_i(\mathbf{r})$.

The next step is to perform the saddle-point approximation with respect to the bosonic fields $\Delta(x_\mu)$, $\Delta^*(x_\mu)$, $\tilde{\rho}_\nu(x_\mu)$, $\rho_\nu(x_\mu)$, which gives the equations,

$$\frac{\delta S}{\delta\Delta^*(x_\mu)} = 0 = \frac{\Delta(x_\mu)}{|U|} - \psi_{s,\downarrow}(x_\mu)\psi_{s,\uparrow}(x_\mu), \tag{A6}$$

$$\frac{\delta S}{\delta\Delta(x_\mu)} = 0 = \frac{\Delta^*(x_\mu)}{|U|} - \psi^*_{s,\uparrow}(x_\mu)\psi^*_{s,\downarrow}(x_\mu), \tag{A7}$$

$$\frac{\delta S}{\delta\tilde{\rho}_\nu(x_\mu)} = 0 = \rho_\nu(x_\mu) - \hat{\rho}_\nu(x_\mu), \tag{A8}$$

$$\frac{\delta S}{\delta \rho_\nu(x_\mu)} = 0 = \int dx'_\mu v_\nu(x_\mu - x'_\mu)\rho_\nu(x'_\mu) + i\tilde{\rho}_\nu(x_\mu). \quad \text{(A9)}$$

The first two equations reproduce the well-known BCS gap equation[33] while the other two give the relationship between ρ_ν, $\tilde{\rho}_\nu$ and the electronic density. These equations provide the starting point for a controlled expansion in terms of Gaussian fluctuations of the bosonic fields around the uniform solutions $\Delta^{(0)}$, $\rho_\nu^{(0)}$, and $\tilde{\rho}_\nu^{(0)}$. In what follows, we assume that the values of $\Delta^{(0)}$, $\rho_\nu^{(0)}$, and $\tilde{\rho}_\nu^{(0)}$ are known. When these solutions are inserted back into the action, Eq. (A5), we notice that the quantity $\tilde{\rho}_\nu^{(0)} = i\rho_\nu^{(0)} \int d^4x_\mu v_\nu(x_\mu)$ can be absorbed in a renormalization of the chemical potential μ_ν due to the effect of Coulomb interactions, while the divergent quantity $\frac{1}{2}\Sigma_{\nu=\pm}(\rho_\nu^{(0)})^2 \int d^4x_\mu d^4x'_\mu v_\nu(x_\mu - x'_\mu)$ exactly cancels the contribution coming from the positive ionic background (which we have not written explicitly here), by imposing the overall electroneutrality of the system, and consequently we will drop it in the following. We also drop the constant term $\beta\Omega\frac{\Delta_0^2}{|U|}$, where Ω is the volume of the superconducting system.

At sufficiently low energies, amplitude fluctuations of the order parameter can be neglected, and we can write $\Delta(x_\mu) = \Delta_0 e^{i\theta(x_\mu)}$, with a real constant $\Delta_0 = |\Delta^{(0)}|$. We can absorb the phase field by the means of a transformation of the fermion field,

$$\psi_{s,\sigma}(x_\mu) \to \psi'_{s,\sigma}(x_\mu) = \psi_{s,\sigma}(x_\mu)e^{i\theta(x_\mu)/2}.$$

The expression of the effective action is considerably simplified introducing the Nambu notation,

$$\mathbf{\Psi}_s(x_\mu) \equiv \begin{pmatrix} \psi_{s,\uparrow}(x_\mu) \\ \psi^*_{s,\downarrow}(x_\mu) \end{pmatrix}, \quad \mathbf{\Psi}_n(x_\mu) \equiv \begin{pmatrix} \psi_{n,\uparrow}(x_\mu) \\ \psi^*_{n,\downarrow}(x_\mu) \end{pmatrix},$$

which allows to write the action as

$$S \simeq \int d^4x_\mu \{\mathbf{\Psi}_s^\dagger[\mathcal{A}_{0,s} - \mathbf{\Sigma}_s]\mathbf{\Psi}_s + \mathbf{\Psi}_n^\dagger[\mathcal{A}_{0,n} - \mathbf{\Sigma}_n]\mathbf{\Psi}_n\}$$
$$+ \frac{1}{2}\sum_\nu \int d^4x_\mu d^4x'_\mu \delta\rho_\nu(x_\mu) v_\nu(x_\mu - x'_\mu)\delta\rho_\nu(x'_\mu)$$
$$+ i\sum_{\nu=\pm} \int d^4x_\mu \delta\tilde{\rho}_\nu(x_\mu)[\rho_\nu^{(0)} + \delta\rho_\nu(x_\mu)],$$

where

$$\delta\tilde{\rho}_\nu(x_\mu) \equiv \tilde{\rho}_\nu(x_\mu) - \tilde{\rho}_\nu^{(0)}, \quad \text{(A10)}$$

$$\delta\rho_\nu(x_\mu) \equiv \rho_\nu(x_\mu) - \rho_\nu^{(0)} \quad \text{(A11)}$$

are the fluctuations of the density around the saddle-point solutions, and

$$\mathcal{A}_{0,s} \equiv \{\partial_\tau\}\hat{\boldsymbol{\tau}}_0 - \left\{\frac{\nabla^2}{2m} + \mu_s\right\}\hat{\boldsymbol{\tau}}_3 - \Delta_0\hat{\boldsymbol{\tau}}_1,$$

$$\mathbf{\Sigma}_s \equiv -\left\{\frac{i(\partial_\tau\theta)}{2} + \frac{(\nabla\theta)^2}{8m} - i\sum_\nu \delta\tilde{\rho}_\nu\right\}\hat{\boldsymbol{\tau}}_3 + \frac{i(\nabla\theta)\nabla}{2m}\hat{\boldsymbol{\tau}}_0,$$

$$\mathcal{A}_{0,n} \equiv \{\partial_\tau\}\hat{\boldsymbol{\tau}}_0 - \left\{\frac{\nabla^2}{2m} + \mu_n\right\}\hat{\boldsymbol{\tau}}_3,$$

$$\mathbf{\Sigma}_n \equiv i\sum_\nu (\nu)\delta\tilde{\rho}_\nu\hat{\boldsymbol{\tau}}_3,$$

where $\hat{\boldsymbol{\tau}}_i$ are the Pauli matrices and where we have used the fact that $\frac{i\nabla\theta[\vec{\nabla}-\vec{\nabla}]}{2m} = \frac{i\nabla\theta\nabla}{m}$ in a translationally invariant system.

The next step consists in using the expansion formula,

$$\mathrm{Tr}\ \ln[\mathcal{A}_0 - \mathbf{\Sigma}] = \mathrm{Tr}\ \ln\ \mathcal{A}_0 - \sum_{n=1}^{\infty}\frac{(-1)^n}{n}\mathrm{Tr}[\mathbf{G}_0\mathbf{\Sigma}]^n,$$

where $\mathbf{G}_0 \equiv -[\mathcal{A}_0]^{-1}$. Truncating the series at second order (i.e., Gaussian fluctuations), we obtain

$$S \simeq -\mathrm{Tr}[\mathbf{G}_{0,s}\mathbf{\Sigma}_s] + \frac{1}{2}\mathrm{Tr}[\mathbf{G}_{0,s}\mathbf{\Sigma}_s]^2 - \mathrm{Tr}[\mathbf{G}_{0,n}\mathbf{\Sigma}_n]$$
$$+ \frac{1}{2}\mathrm{Tr}[\mathbf{G}_{0,n}\mathbf{\Sigma}_n]^2 + \frac{1}{2}\sum_\nu \int d^4x_\mu d^4x'_\mu \delta\rho_\nu(x_\mu) v_\nu(x_\mu$$
$$- x'_\mu)\delta\rho_\nu(x'_\mu) + i\sum_{\nu=\pm} \int d^4x_\mu \delta\tilde{\rho}_\nu(x_\mu)[\rho_\nu^{(0)} + \delta\rho_\nu(x_\mu)],$$

where the propagators in Nambu space $\mathbf{G}_{0,s}$ and $\mathbf{G}_{0,n}$ write

$$\mathbf{G}_{0,s} = \begin{pmatrix} g_{0,s}(x_\mu) & f_{0,s}(x_\mu) \\ \bar{f}_{0,s}(x_\mu) & \bar{g}_{0,s}(x_\mu) \end{pmatrix},$$

$$\mathbf{G}_{0,n} = \begin{pmatrix} g_{0,n}(x_\mu) & 0 \\ 0 & \bar{g}_{0,n}(x_\mu) \end{pmatrix},$$

and where $g_{0,s}(x_\mu) \equiv -\langle T_\tau \psi_{s,\uparrow}(x_\mu)\psi^*_{s,\uparrow}(0)\rangle$ and $\bar{g}_{0,s}(x_\mu) \equiv \langle T_\tau \psi^*_{s,\downarrow}(x_\mu)\psi_{s,\downarrow}(0)\rangle$ denote, respectively, the particle and hole propagators in the superconductor, while $f_{0,s}(x_\mu) \equiv \langle T_\tau \psi_{s,\downarrow}(x_\mu)\psi_{s,\uparrow}(0)\rangle$, $\bar{f}_{0,s}(x_\mu) \equiv \langle T_\tau \psi^*_{s,\uparrow}(x_\mu)\psi^*_{s,\downarrow}(0)\rangle$ are the anomalous ones.[64] Similarly $g_{0,n}(x_\mu) \equiv -\langle T_\tau \psi_{n,\uparrow}(x_\mu)\psi^*_{n,\uparrow}(0)\rangle$ and $\bar{g}_{0,n}(x_\mu) \equiv \langle T_\tau \psi^*_{n,\downarrow}(x_\mu)\psi_{n,\downarrow}(0)\rangle$ are the particle and hole propagators in the normal metal, respectively.

The evaluation of the traces yields

$$\mathrm{Tr}[\mathbf{G}_{0,s}\mathbf{\Sigma}_s] = -\rho_s^{(0)} \int d^4x_\mu \left[\frac{i}{2}\partial_\tau\theta + \frac{(\nabla\theta)^2}{8m} - i\sum_\nu \delta\tilde{\rho}_\nu\right]_{x_\mu},$$

$$\mathrm{Tr}[\mathbf{G}_{0,s}\mathbf{\Sigma}_s]^2 = \int d^4x_\mu d^4x'_\mu \Bigg\{\chi_{0,s}(x_\mu - x'_\mu)$$
$$\times \left[\frac{1}{2}\partial_\tau\theta - \sum_\nu \delta\tilde{\rho}_\nu\right]_{x_\mu}\left[\frac{1}{2}\partial_\tau\theta - \sum_{\nu'} \delta\tilde{\rho}_{\nu'}\right]_{x'_\mu}$$
$$- \mathcal{D}'(x_\mu - x'_\mu)[\nabla\theta]_{x_\mu}[\nabla\theta]_{x'_\mu}\Bigg\},$$

$$\mathrm{Tr}[\mathbf{G}_{0,n}\mathbf{\Sigma}_n] = i\rho_n^{(0)} \int d^4x_\mu \left[\sum_\nu (\nu)\delta\tilde{\rho}_\nu\right]_{x_\mu},$$

$$\mathrm{Tr}[\mathbf{G}_{0,n}\mathbf{\Sigma}_n]^2 = \int d^4x_\mu d^4x'_\mu \chi_{0,n}(x_\mu - x'_\mu) \times \left[\sum_\nu (\nu)\delta\tilde{\rho}_\nu\right]_{x_\mu}\left[\sum_{\nu'}(\nu')\delta\tilde{\rho}_{\nu'}\right]_{x'_\mu},$$

where for simplicity we have used the compact notation $[\mathcal{O}]_{x_\mu} \equiv \mathcal{O}(x_\mu)$, and where we have defined

$$\mathcal{D}'(x_\mu - x'_\mu) \equiv \frac{1}{2m^2}[\nabla g_{0,s}(x'_\mu - x_\mu)\,\nabla\, g_{0,s}(x_\mu - x'_\mu) + \nabla f_{0,s}(x'_\mu - x_\mu)\,\nabla\, f_{0,s}(x_\mu - x'_\mu)]$$

and the density-density correlation functions

$$\chi_{0,s}(x_\mu - x'_\mu) \equiv -\langle T_\tau \delta\rho_s(x_\mu)\delta\rho_s(x'_\mu)\rangle = -2g_{0,s}(x_\mu - x'_\mu)g_{0,s}(x'_\mu - x_\mu) + 2f_{0,s}(x_\mu - x'_\mu)f_{0,s}(x'_\mu - x_\mu), \quad \text{(A12)}$$

$$\chi_{0,n}(x_\mu - x'_\mu) \equiv -\langle T_\tau \delta\rho_n(x_\mu)\delta\rho_n(x'_\mu)\rangle = -2g_{0,n}(x_\mu - x'_\mu)g_{0,n}(x'_\mu - x_\mu). \quad \text{(A13)}$$

The final step is to integrate out the modes $\delta\tilde{\rho}_\nu(x_\mu)$. To that aim, we decouple the mixed term $\sim(\delta\tilde{\rho}_\nu)(\delta\tilde{\rho}_{\bar{\nu}})'$ appearing in $\mathrm{Tr}[\mathbf{G}_{0,s}\mathbf{\Sigma}_s]^2$ and $\mathrm{Tr}[\mathbf{G}_{0,n}\mathbf{\Sigma}_n]^2$ by returning to the original representation for the densities [cf. Eq. (7)],

$$\delta\tilde{\rho}_s = \frac{\delta\tilde{\rho}_+ + \delta\tilde{\rho}_-}{2},$$

$$\delta\tilde{\rho}_n = \frac{\delta\tilde{\rho}_+ - \delta\tilde{\rho}_-}{2},$$

and integrate out the fields $\delta\tilde{\rho}_n(x_\mu)$ and $\delta\tilde{\rho}_s(x_\mu)$ instead. From here we see that the term $\sim(\partial_\tau\theta)(\partial_\tau\theta)'$ cancels, as in Ref. 21. We finally obtain

$$S = \frac{i}{2}\int d^4x_\mu \partial_\tau\theta(x_\mu)\rho_s(x_\mu) + \int d^4x_\mu d^4x'_\mu \left\{\frac{1}{2}\mathcal{D}(x_\mu - x'_\mu)\,\nabla\,\theta(x_\mu)\,\nabla\,\theta(x'_\mu) + \boldsymbol{\delta\rho}^\dagger(x_\mu)\hat{\boldsymbol{\chi}}^{-1}(x_\mu - x'_\mu)\boldsymbol{\delta\rho}(x'_\mu)\right\}, \quad \text{(A14)}$$

where we have defined

$$\mathcal{D}(x_\mu) \equiv \frac{\rho_s^{(0)}}{4m}\delta(x_\mu) - \mathcal{D}'(x_\mu),$$

$$\boldsymbol{\delta\rho}(x_\mu) \equiv \begin{pmatrix}\delta\rho_s(x_\mu)\\ \delta\rho_n(x_\mu)\end{pmatrix},$$

$$\hat{\boldsymbol{\chi}}^{-1}(x_\mu) \equiv \begin{pmatrix}[\chi_{0,s}(x_\mu)]^{-1} & 0\\ 0 & [\chi_{0,n}(x_\mu)]^{-1}\end{pmatrix} + \delta(\tau) \times \begin{pmatrix} v(x_\mu,0) & v(x_\mu,d)\\ v(x_\mu,d) & v(x_\mu,0)\end{pmatrix}, \quad \text{(A15)}$$

where the compact notation of Eq. (A3) has been used for $[\chi_{0,a}(x_\mu)]^{-1}$.

APPENDIX B: DENSITY SUSCEPTIBILITY AND SUPERCONDUCTING STIFFNESS IN THE LIMIT $q^\mu \to 0$

From Eq. (A12), the Fourier transforms reads

$$\chi_{0,s}(q^\mu) = \frac{2}{\beta\Omega}\sum_{k^\mu}[-g_{0,s}(k^\mu)g_{0,s}(k^\mu - q^\mu) + f_{0,s}(k^\mu)f_{0,s}(k - q^\mu)].$$

In the limit $q^\mu \to 0$, we obtain

$$\lim_{q^\mu\to 0}\chi_{0,s}(q^\mu) \to -\frac{2}{\Omega}\sum_{\mathbf{k}}\frac{1}{\beta}\sum_n \frac{(i\nu_n)^2 + \xi_{\mathbf{k}}^2 - \Delta_0^2}{[(i\nu_n)^2 - E_{\mathbf{k}}^2]^2} = -\frac{2}{\Omega}\left[\sum_k \frac{n_F(E_{\mathbf{k}})}{2E_{\mathbf{k}}} - \frac{n_F(-E_{\mathbf{k}})}{2E_{\mathbf{k}}}\right]$$

with $\xi_{\mathbf{k}} \equiv \frac{k^2}{2m} - \mu_s$ and $E_{\mathbf{k}} \equiv \sqrt{\xi_{\mathbf{k}}^2 + \Delta_0^2}$. At $T=0$,

$$\lim_{q^\mu\to 0}\chi_{0,s}(q^\mu) = \frac{2}{\Omega}\sum_{\mathbf{k}}\frac{1}{2E_{\mathbf{k}}} = \mathcal{N}_s^{(0)}\gamma, \quad \text{(B1)}$$

where $\gamma \equiv \int_{-\omega_D}^{\omega_D} d\xi \frac{1}{\sqrt{\xi^2+\Delta_0^2}} = \ln\left[\frac{\omega_D + \sqrt{\omega_D^2+\Delta_0^2}}{-\omega_D + \sqrt{\omega_D^2+\Delta_0^2}}\right] \approx 2\ln\left[\frac{2\omega_D}{\Delta_0}\right]$, and where ω_D is a high-energy cutoff.

Similarly, the Fourier transform of the superconducting stiffness reads

$$\mathcal{D}(q^\mu) \equiv \frac{\rho_s^{(0)}}{4m} - \mathcal{D}'(q^\mu)$$

with

$$\mathcal{D}'(q^\mu) \equiv \frac{1}{\Omega}\sum_{k^\mu} \frac{-\mathbf{k}\cdot(\mathbf{k}-\mathbf{q})}{2m^2} \times[f(k^\mu)f(k^\mu-q^\mu)+g(k^\mu)g(k^\mu-q^\mu)]$$
$$= \frac{1}{V}\sum_{\mathbf{k}} \frac{-\mathbf{k}\cdot(\mathbf{k}-\mathbf{q})}{2m^2} \times \frac{1}{\beta}\sum_n \frac{\Delta_0^2+(i\nu_n+\xi_{\mathbf{k}})(i\nu_n-i\omega_m+\xi_{\mathbf{k}-\mathbf{q}})}{[(i\nu_n)^2-E_{\mathbf{k}}^2][(i\nu_n-i\omega_m)^2-E_{\mathbf{k}-\mathbf{q}}^2]}.$$

Evaluating the Matsubara sum over the fermionic frequencies $i\nu_n$, we obtain the result in the limit $q^\mu \to 0$,

$$\lim_{q^\mu\to 0}\mathcal{D}'(q^\mu) \approx -\frac{1}{V}\sum_{\mathbf{k}} \frac{k^2}{2m^2}\frac{n_F(E_{\mathbf{k}})-n_F(E_{\mathbf{k}-\mathbf{q}})}{E_{\mathbf{k}}-E_{\mathbf{k}-\mathbf{q}}} \approx -\frac{1}{V}\sum_{\mathbf{k}} \frac{k^2}{2m^2}\frac{\partial n_F(E_{\mathbf{k}})}{\partial E_{\mathbf{k}}},$$

which vanishes in the limit $T\to 0$, and we recover the well-know result,[33,64]

$$\lim_{q^\mu\to 0}\mathcal{D}(q^\mu) \equiv \mathcal{D}_0 = \frac{\rho_s^{(0)}}{4m}.$$

[1] A. O. Caldeira and A. J. Leggett, Ann. Phys. **149**, 374 (1983).
[2] S. Chakravarty, Phys. Rev. Lett. **49**, 681 (1982).
[3] A. J. Bray and M. A. Moore, Phys. Rev. Lett. **49**, 1545 (1982).
[4] A. Schmid, Phys. Rev. Lett. **51**, 1506 (1983).
[5] B. G. Orr, H. M. Jaeger, A. M. Goldman, and C. G. Kuper, Phys. Rev. Lett. **56**, 378 (1986).
[6] D. B. Haviland, Y. Liu, and A. M. Goldman, Phys. Rev. Lett. **62**, 2180 (1989).
[7] L. J. Geerligs, M. Peters, L. E. M. de Groot, A. Verbruggen, and J. E. Mooij, Phys. Rev. Lett. **63**, 326 (1989).
[8] E. G. Dalla Torre, E. Demler, T. Giamarchi, and E. Altman, arXiv:0908.0868, Nature Phys. (to be published).
[9] A. G. Sun, L. M. Paulius, D. A. Gajewski, M. B. Maple, and R. C. Dynes, Phys. Rev. B **50**, 3266 (1994).
[10] J. E. Mooij and G. Schön, Phys. Rev. Lett. **55**, 114 (1985).
[11] T. Giamarchi, *Quantum Physics in One Dimension* (Oxford University Press, Oxford, 2004).
[12] A. D. Zaikin, D. S. Golubev, A. van Otterlo, and G. T. Zimányi, Phys. Rev. Lett. **78**, 1552 (1997).
[13] H. P. Büchler, V. B. Geshkenbein, and G. Blatter, Phys. Rev. Lett. **92**, 067007 (2004).
[14] P. Goswami and S. Chakravarty, Phys. Rev. B **73**, 094516 (2006).
[15] G. Refael, E. Demler, Y. Oreg, and D. S. Fisher, Phys. Rev. B **75**, 014522 (2007).
[16] A. Bezryadin, C. N. Lau, and M. Tinkham, Nature (London) **404**, 971 (2000).
[17] C. N. Lau, N. Markovic, M. Bockrath, A. Bezryadin, and M. Tinkham, Phys. Rev. Lett. **87**, 217003 (2001).
[18] F. Altomare, A. M. Chang, M. R. Melloch, Y. Hong, and C. W. Tu, Phys. Rev. Lett. **97**, 017001 (2006).
[19] A. Vishwanath, J. E. Moore, and T. Senthil, Phys. Rev. B **69**, 054507 (2004).
[20] D. M. Gaitonde, Int. J. Mod. Phys. B **12**, 2717 (1998).
[21] S. De Palo, C. Castellani, C. Di Castro, and B. K. Chakraverty, Phys. Rev. B **60**, 564 (1999).
[22] A. J. Rimberg, T. R. Ho, Ç. Kurdak, J. Clarke, K. L. Campman, and A. C. Gossard, Phys. Rev. Lett. **78**, 2632 (1997).
[23] J. González and E. Perfetto, Phys. Rev. B **72**, 205406 (2005).
[24] M. A. Cazalilla, F. Sols, and F. Guinea, Phys. Rev. Lett. **97**, 076401 (2006).
[25] H. C. Fu, A. Seidel, J. Clarke, and D.-H. Lee, Phys. Rev. Lett. **96**, 157005 (2006).
[26] A. M. Lobos, A. Iucci, M. Müller, and T. Giamarchi, Phys. Rev. B **80**, 214515 (2009).
[27] G. Liu, Y. Zhang, and C. N. Lau, Phys. Rev. Lett. **102**, 016803 (2009).
[28] Y. Chen, S. D. Snyder, and A. M. Goldman, Phys. Rev. Lett. **103**, 127002 (2009).
[29] V. Ambegaokar, U. Eckern, and G. Schön, Phys. Rev. Lett. **48**, 1745 (1982).
[30] A. van Otterlo, D. S. Golubev, A. Zaikin, and G. Blatter, Eur. Phys. J. B **10**, 131 (1999).
[31] J. W. Negele and H. Orland, *Quantum Many Particle Systems* (Addison-Wesley, Reading, 1987).
[32] G. D. Mahan, *Many-Particle Physics*, Physics of Solids and Liquids, 3rd ed. (Kluwer Academic/Plenum, New York, 2000).
[33] M. Tinkham, *Introduction to Superconductivity*, 2nd ed. (McGraw-Hill, New York, 1996).
[34] M. Abramowitz and I. Stegun, *Handbook of Mathematical Functions* (Dover, New York, 1972).
[35] A. M. Kadin, *Introduction to Superconducting Circuits* (Wiley, New York, 1999).
[36] J. S. Langer and V. Ambegaokar, Phys. Rev. **164**, 498 (1967).
[37] D. E. McCumber and B. I. Halperin, Phys. Rev. B **1**, 1054 (1970).
[38] T. Giamarchi, Phys. Rev. B **46**, 342 (1992).
[39] N. Giodano, Physica B **203**, 460 (1994).
[40] K. Y. Arutyunov, D. S. Golubev, and A. D. Zaikin, Phys. Rep. **464**, 1 (2008).
[41] J. M. Kosterlitz and D. J. Thouless, J. Phys. C **6**, 1181 (1973).
[42] N. D. Mermin and H. Wagner, Phys. Rev. Lett. **17**, 1133 (1966).
[43] H. J. Schulz, Phys. Rev. Lett. **71**, 1864 (1993).
[44] E. Akkermans and G. Montambaux, *Mesoscopic Physics of Electrons and Photons* (Cambridge University Press, Cambridge, 2007).
[45] S. Chakravarty, G.-L. Ingold, S. Kivelson, and A. Luther, Phys. Rev. Lett. **56**, 2303 (1986).
[46] S. Chakravarty, G.-L. Ingold, S. Kivelson, and G. Zimanyi, Phys. Rev. B **37**, 3283 (1988).
[47] R. Fazio and H. van der Zant, Phys. Rep. **355**, 235 (2001).
[48] A. H. Castro Neto, C. de C. Chamon, and C. Nayak, Phys. Rev. Lett. **79**, 4629 (1997).
[49] Note, however, that in general is technically difficult to have complete experimental access to $\sigma(k_\parallel,\omega)$ as a function of $k_\parallel$ and

ω since, typically, optical measurements allow only to measure $\sigma(k_{\|}=0,\omega)$.

[50] K. S. Takahashi, M. Gabay, D. Jaccard, K. Shibuya, T. Ohnishi, M. Lippmaa, and J. M. Triscone, Nature (London) **441**, 195 (2006).

[51] N. Reyren *et al.*, Science **317**, 1196 (2007).

[52] A. D. Caviglia, S. Gariglio, N. Reyren, D. Jaccard, T. Schneider, M. Gabay, S. Thiel, G. Hammerl, J. Mannhart, and J. M. Triscone, Nature (London) **456**, 624 (2008).

[53] A. G. Rojo, J. Phys.: Condens. Matter **11**, R31 (1999).

[54] J.-M. Duan and S. Yip, Phys. Rev. Lett. **70**, 3647 (1993).

[55] M. Pustilnik, E. G. Mishchenko, L. I. Glazman, and A. V. Andreev, Phys. Rev. Lett. **91**, 126805 (2003).

[56] K. Flensberg, Phys. Rev. Lett. **81**, 184 (1998).

[57] Y. V. Nazarov and D. V. Averin, Phys. Rev. Lett. **81**, 653 (1998).

[58] R. Klesse and A. Stern, Phys. Rev. B **62**, 16912 (2000).

[59] N. Giordano and J. D. Monnier, Phys. Rev. B **50**, 9363 (1994).

[60] X. Huang, G. Bazàn, and G. H. Bernstein, Phys. Rev. Lett. **74**, 4051 (1995).

[61] L. A. Farina, K. M. Lewis, C. Kurdak, S. Ghosh, and P. Bhattacharya, Phys. Rev. B **70**, 153302 (2004).

[62] A. R. Goñi, A. Pinczuk, J. S. Weiner, J. M. Calleja, B. S. Dennis, L. N. Pfeiffer, and K. W. West, Phys. Rev. Lett. **67**, 3298 (1991).

[63] O. Buisson, F. Parage, B. Camarota, T. Henning, I. Wooldridge, and P. Delsing, Physica B **284-288**, 1740 (2000).

[64] A. L. Fetter and J. D. Walecka, *Quantum Theory of Many-Particle Systems* (McGraw-Hill, New York, 1971).